

MULTICOLOR PHOTOMETRY OF THE GALAXIES IN ABELL 2255 BY THE BATC AND SDSS SURVEYS

Qirong Yuan^{1,2}, Xu Zhou², and Zhaoji Jiang²

ABSTRACT

We present our optical multicolor photometry for the nearby cluster of galaxies Abell 2255 with 13 intermediate filters in the Beijing-Arizona-Taiwan-Connecticut (BATC) system which cover an optical wavelength range from 3000 to 10000 Å. The spectral energy distributions (SEDs) in the optical band for more than 7000 sources are achieved down to $V \sim 20$ in a field of $58' \times 58'$ centered on this rich cluster. Abell 2255 has been recently observed by the Sloan Digital Sky Survey (SDSS) down to $V \sim 17.5$ spectroscopically and $r' \sim 22.0$ photometrically. A method of combining the SDSS photometric data in five broad bands and the BATC SEDs is then explored. A sample of 254 galaxies with known redshifts in the region of Abell 2255 is constructed for testing the reliability of the method of combining SEDs. Our application of the technique of photometric redshift on this sample shows that the combined SEDs with higher resolution could lead to a more accurate estimate of photometric redshift. Based on 214 spectroscopically confirmed member galaxies, spatial and dynamical properties of this cluster are studied. Bimodality and large dispersion in the velocity distribution indicate that Abell 2255 is an unrelaxed system. A tight color-magnitude correlation for 188 known early-type cluster galaxies is found. After an exclusion of 254 extragalactic sources with known redshifts, the combined SEDs for 2522 galaxies allow a further membership selection by the photometric redshift technique and color-magnitude correlation. As a result, 313 galaxies with their photometric redshifts between 0.068 and 0.090 are selected as new cluster members. The combined SEDs and estimated redshifts for previously known and newly-selected member galaxies are cataloged. On the basis of the enlarged sample of member galaxies, the spatial distribution, localized velocity structure, color-magnitude relation, and luminosity function of cluster galaxies are discussed. The reverse peculiar velocities are found for two satellite subclusters located on opposite sides of the central concentration, which supports an ongoing merger in Abell 2255.

Subject headings: galaxies: clusters: individual (Abell 2255) — galaxies: distances and redshifts — galaxies: kinematics and dynamics — methods: data analysis

¹Department of Physics, Nanjing Normal University, NingHai Road 122, Nanjing 210097, China;
qryuan@email.njnu.edu.cn

²National Astronomical Observatories, Chinese Academy of Sciences, Beijing 100012, China

1. INTRODUCTION

As the largest gravitationally bound systems in the Universe, galaxy clusters have been attracting more and more observational efforts in the last decade. According to the hierarchical models for large-scale structure formation in the picture of cold dark matter, galaxy clusters are built up by the process of hierarchical clustering in which larger clusters are formed by the coalescence of smaller clusters. Strong gravitational encounters between galaxy clusters are essential in forming the structures we observe today. This scenario is supported by the recent X-ray observations of some nearby rich clusters which give convincing evidence for a ongoing merger event (Colless & Dunn 1996). The rich cluster of galaxies, Abell 2255, is one of the well-studied examples.

The nearby galaxy cluster Abell 2255 has recently been observed in radio, optical, and X-ray bands, and a complicated picture of its dynamics, structure of the member galaxies, and intergalactic medium is unveiled. From its radio maps at 20 cm, a diffuse halo source appears at the cluster center, and 6 tailed radio sources are found to be associated with cluster galaxies (Feretti et al 1997). The electrons can be accelerated throughout the cluster to power a radio halo in the outer region if this cluster is undergoing a merger (Tribble 1993). The asymmetric structure in Abell 2255 detected by ROSAT imaging observations and the nonisothermal temperature map of the intracluster gas in this cluster support the discovery of a currently undergoing merger (Davis & White 1998). From the optical point of view, there are two comparably bright galaxies near the cluster center, which is thought to be the evidence of recent merger events with two less massive systems of galaxies (Bird 1994). This scenario is also supported by the unusually large radial velocity dispersion of $\sim 1221 \text{ km s}^{-1}$, which may be indicative of the dynamically unrelaxed phase (Zabludoff et al. 1990). Furthermore, the optical images show that the X-ray emission centroid does not coincide with any bright galaxy or galaxy subgroup (Burns et at. 1995). These intriguing observational features may tell us that this cluster is not a simple relaxed structure, but is still forming at the present epoch.

However, no obvious evidences of spatial or kinematical substructure in Abell 2255 was found in optical band (Stauffer et al. 1979; Zabludoff et al. 1990). It is mainly because only the limited number of cluster galaxies brighter than $V \sim 16.0$ have been spectroscopically observed a decade ago. Recently, accurate photometric data for the objects in this cluster were obtained and distributed by the Sloan Digital Sky Survey (SDSS). However, the SDSS spectroscopic survey covers merely the galaxies brighter than $V \sim 18.0$. Based on the luminosity function of cluster galaxies (Lobo, et al. 1997), a typical galaxy with $M_V \sim -18.0$ has an apparent magnitude of $V \sim 20.5$, fainter than the limit of the SDSS spectroscopic survey. For a better understanding of structure and dynamics of this cluster, the faint member galaxies ($18.0 < m_v < 21.5$) should be taken into account. This paper will present our optical photometry of the galaxies in Abell 2255 with the Beijing-Arizona-Taiwan-Connecticut (hereafter BATC) multicolor system. The BATC multicolor photometric survey aims mainly at obtaining the spectral energy distribution (SED) information of galaxies with redshift less than 0.5 (Xia et al. 2002), by using the 60/90 cm Schmidt Telescope of Beijing Astronomical Observatory (BAO) with 15 intermediate-band filters. Our previous work shows that the multicolor

photometry with 1-meter class Schmidt Telescope can provide the SED information for all the objects within a large field of view ($\sim 1 \text{ deg}^2$) centered on a nearby galaxy cluster, which will facilitate the follow-up investigations on membership selection and the color-magnitude relation (Yuan et al. 2001). Since the accuracy of photometric redshifts is heavily dependent upon the number of filters (i.e., spectral resolution) and the photometric accuracy in each band (Xia et al. 2002), the SDSS photometric data in five photometric bands (Fukugita et al. 1996) will be combined with the BATC SEDs for all the objects detected within our field. Current study will result in an SED catalog of not only previously known (bright) member galaxies but the newly-selected faint members. Based on the enlarged sample of cluster galaxies, the spatial distribution, dynamics, color properties and luminosity function of cluster galaxies in Abell 2255 can be then addressed.

The structure of this paper is as follows. In §2, we present the BATC multicolor photometric observations and data reduction, as well as the cross-identification between the BATC and SDSS photometric catalogs. The methodology of combining the SDSS SEDs with the BATC SEDs are detailed in §3. The analysis of SED features for the previously known member galaxies is shown in §4, and the combined SEDs of known galaxies in Abell 2255 are also cataloged. The further SED selection of faint members is given in §5. The dynamical and color properties of the enlarged sample of cluster galaxies is presented in §6, as well as the luminosity function of cluster galaxies. Finally, we give a summary in §7. The cosmological parameters $H_0=50 \text{ km s}^{-1} \text{ Mpc}^{-1}$ and $q_0=0.5$ are assumed throughout this paper.

2. OBSERVATIONS AND DATA REDUCTION

Abell 2255 is a nearby ($z \sim 0.0806$, giving a distance modulus of 38.3; Struble & Rood 1999) cluster of galaxies with richness class 2 in Abell (1958), classified as a type II-III cluster by Bautz & Morgan (1970). The BATC photometric observations of Abell 2255 were taken with the 60/90 cm f/3 Schmidt Telescope of BAO, located at the Xinglong site with an altitude of 900m. A Ford 2048 \times 2048 CCD camera was equipped at the prime focus of the telescope. The field of view was ~ 1.0 square degree, and the spatial scale was $1.7''$ per pixel. The combined image in each filter covers a sky region of $59 \times 59 \text{ arcmin}^2$, defined by a right ascension range from $17^h 08^m 03^s.7$ to $17^h 16^m 58^s.6$, and a declination range from $63^\circ 36' 31''.5$ to $64^\circ 35' 28''.8$ (for equinox of 2000.0). The BATC filter system includes 15 intermediate-band filters, namely, $a-k$, $m-p$, covering the whole optical wavelength range from ~ 3000 to 10000 \AA . The details of the BAO Schmidt Telescope, CCD camera and data-acquisition system can be found elsewhere (Fan et al. 1996; Yan et al. 2000). For distinguishing explicitly between the SDSS and BATC filter names, in this paper we refer the SDSS filters and magnitudes to as u' , g' , r' , i' , and z' , which corresponds to central wavelengths of 3560, 4680, 6180, 7500 and 8870 \AA . The transmissions of the BATC and SDSS filters can be seen in Fig. 1.

Fig. 1: The transmissions of the BATC and SDSS filters

Only 13 BATC filters were used for the multicolor imaging observations of Abell 2255. In total,

we have made more than 40 *hr* of exposures. After a check of the image quality, 113 images with more than 36 *hr* of exposure were selected to be combined. The parameters of the BATC filters we used and the observational details are given in Table 1. The bias subtractions and dome flat-field corrections were done on the CCD images, using *Pipeline 1*, the automatic data reduction code for the BATC survey. The cosmic ray and bad pixel effect were corrected by comparing the images. Before combination, the images were re-centered and position calibration was performed by using the Guide Star Catalog (GSC). The processes of the point spread function (PSF) fitting and the aperture photometries with different apertures were performed for the objects detected in the images of at least 3 filter bands, using the code named as *Pipeline 2* (Zhou, et al. 2003). As a result, the list of PSF and aperture magnitudes in various filter bands was obtained for all the objects detected. For the bright galaxies in the region of Abell 2255, we adopted the aperture magnitudes defined by a fixed aperture with a radius of 4 pixels (i.e., 6.8 arcsec) which is large enough to make different seeing effects negligible. Although the magnitudes measured with a fixed aperture are not the same as the total magnitudes of galaxies in the literature, this is a proper way to obtain the reliable color indices (i.e., relative SEDs) of all the objects. Since the adopted aperture size is rather large, contamination of the light by nearby objects may sometimes not be negligible. The number of sources detected in the combined images are shown in Table 1, along with the details of the observations.

Table 1: The details of the BATC filters and our observations

No.	Filter name	λ_{eff} (Å)	FWHM (Å)	Exposure (second)	Number of Images	Seeing ^a (arcsec)	Objects Detected	Limiting mag
1	b	3907	291	10800	9	4.74	5678	20.5
2	d	4540	332	13200	11	5.45	6816	20.5
3	e	4925	374	12000	10	4.32	7227	20.0
4	f	5267	344	11400	10	4.98	7253	20.0
5	g	5790	289	7200	6	3.96	7337	20.0
6	h	6074	308	6950	7	4.18	7319	20.0
7	i	6656	491	12900	12	4.61	6884	19.5
8	j	7057	238	4800	4	4.36	7437	20.0
9	k	7546	192	4800	4	4.62	7386	19.0
10	m	8023	255	14400	12	4.11	7368	19.0
11	n	8484	167	9600	8	5.13	7047	19.0
12	o	9182	247	12000	10	3.81	7355	18.5
13	p	9739	275	12000	10	4.21	6796	18.5

^a This column lists the seeings of the combined images.

To obtain the *relative* SEDs of objects in this field, the model calibration was made for the combined images. This method was developed to calibrate the SEDs of objects in a large field of view on the basis of the SED library, especially for the BATC multicolor photometric system (Zhou et al.

1999). No calibration images of the standard stars are needed to derive the relative SEDs.

It can be expected that the SDSS photometric data can be used to do flux calibration of the BATC SEDs, which will be described in next section. Therefore we cross-identified all the sources detected by both photometric observations. All the sources in the BATC catalog within the searching circle (defined by a radius of 2.0 arcsec) centered on the SDSS sources were extracted. By comparing the SED features, the identification was rather unambiguous. According to the morphology classification given in the SDSS photometric catalog, 3651 point sources (stars) and 2790 extended sources (galaxies) were found in both surveys. Furthermore, we extracted the BATC and SDSS photometric information for all known extragalactic objects listed in the NASA/IPAC Extragalactic Database (NED). There are 340 known sources in our observation field, among which 274 (81%) are galaxies and 14 (4%) are quasars. The remainder are sources that appear only in one of surveys from radio, infrared, X-ray, and γ -ray wavebands. Some 254 galaxies have been found to have NED-given spectroscopic redshifts. The counterparts for those 254 galaxies with known spectroscopic redshifts were found in both of the BATC and SDSS imaging observations, which offers a good sample for our further analyses.

3. METHOD OF COMBINING THE SDSS AND BATC SEDS

It is clear that combination of the BATC SEDs with the SDSS photometric data will lead to a more accurate estimate of photometric redshift. Therefore we tried to derive the SDSS colors of galaxies through the same aperture as defined by the BATC photometry (i.e., aperture radius $r_{ap} = 4 \times 1.7 = 6.8$ arcsec), using the photometric parameters provided by the SDSS Early Data Release (EDR; Stoughton et al. 2002). The SDSS imaging observations of Abell 2255 were carried out by drift scanning with a spatial scale of 0.4 arcsec pix $^{-1}$ in five broad bandpasses. The effective integration time was 54 seconds, and all images were reduced with software specially designed for the SDSS data (Lupton et al. 2001).

3.1. Aperture Correction of the SDSS Photometries for Galaxies

For a given bright galaxy detected by the SDSS imaging observation, the observed profile of surface brightness is quantified by some global photometric parameters, such as the likelihood parameters for various models, the effective radius (r_e) along the major axis, and the *model* magnitude (m_{model}) which represents the total magnitude estimated by the optimum model in the r' band. The three following models were used to fit the observed surface-brightness profile: (i) the point spread function (PSF) model, (ii) de Vaucouleurs (1948) $r^{1/4}$ model, and (iii) exponential model. The model magnitudes in other four bands were calculated using the effective radius defined by the preferential modelling in the r' band. Some studies show that the de Vaucouleurs model appears to be a very good fit to the elliptical galaxies' surface-brightness (de Vaucouleurs & Capaccioli 1979; Capaccioli et al. 1990). The difference between the *model* magnitude (m_{model}) and the magnitude within a given aperture (m_{ap})

can be derived by

$$\Delta m = m_{ap} - m_{model} = -2.5 \log \frac{\int_0^{r_{ap}} 2\pi r I(r) dr}{\int_0^{\infty} 2\pi r I(r) dr}, \quad (1)$$

where $I(r)$ is the profile function of surface intensity defined as

$$I(r) = \begin{cases} I_0 \exp\{-7.67[(r/r_e)^{1/4}]\}, & \text{as } 0 < r \leq 7r_e, \\ a_0 I_0(8 - r/r_e), & \text{as } 7r_e < r < 8r_e. \end{cases} \quad (2)$$

for the de Vaucouleurs $r^{1/4}$ model, or

$$I(r) = \begin{cases} I_0 \exp(-1.68 r/r_e), & \text{as } 0 < r \leq 3r_e, \\ b_0 I_0(4 - r/r_e), & \text{as } 3r_e < r < 4r_e. \end{cases} \quad (3)$$

for the exponential model, where the dimensionless quantities a_0 and b_0 are intensities relative to the amplitude I_0 at $7r_e$ and $3r_e$, respectively: $a_0 = 3.8178 \times 10^{-6}$ and $b_0 = 6.4737 \times 10^{-3}$. The aperture correction Δm is the same for the *model* magnitudes in five SDSS filters, since the model with higher likelihood in the r' filter is selected to be used in the other bands with the same effective radius r_e for a specific object, allowing only the amplitude I_0 to vary.

It is well known that the vast majority of stars detected in the BATC observations have the brightness profiles which can be well modelled by the point spread function (PSF). Therefore we adopted the PSF magnitudes in the BATC and SDSS observations as optimal measures of the fluxes of stars.

3.2. Flux Calibration of the BATC SEDs

The SDSS model magnitudes are flux-calibrated by comparison with a set of overlapping standard-star fields calibrated with a 0.5-m “photometric Telescope”. The uncertainties of the model magnitudes are also listed in the SDSS EDR photometric catalog. In general, the error for u' model magnitude is larger than those in other bands, and brighter sources have less fitting uncertainties. For a known galaxy having $u' < 19.5$, the typical u' error is less than 0.1.

As we mentioned above, the BATC SEDs were calibrated by comparing with the SED library of bright stars in the BATC field. After the model calibrations, the relative SEDs for all the objects in the BATC photometric field were obtained. The zero-point of the BATC SEDs of galaxies can be determined by the aperture-corrected SDSS SEDs. Fig. 2 shows the relative SEDs in the BATC and SDSS multicolor systems for SDSS J171236.07+640508.0, the central early-type galaxy in Abell 2255 cluster. The zero-point of the BATC SEDs can be derived simply by averaging the magnitude differences at 6166 and 7480 Å, the effective wavelengths of r' and i' filters. The interpolation can be used to derive the BATC magnitudes at 6166 and 7480 Å, based on the magnitudes in the neighboring BATC bands. The flux zero-points for different galaxies are slightly different, since the deviation of the surface-brightness profile from the preferential model is different from source to source.

In calculation of flux zero-point for each star, we directly used the PSF magnitudes measured in BATC and SDSS images. No aperture corrections are needed for the SDSS magnitudes of stars. The average value of magnitude differences at 6166 and 7480 Å is also defined as the flux zero-point for each star. We present the zero-point distribution for all the stars and galaxies detected by both multicolor surveys in Fig. 3. It can be seen that the stars have more concentrated distribution of SED zero-points (thick line), with a peak at 3.24. A wider range of fitting deviations for galaxies leads to a comparatively scattered zero-point distribution (thin line) with the same typical zero-point.

Fig. 2: BATC and SDSS SEDs for SDSS J171236.07+640508.0

Fig. 3: Zero-point distribution

As a result, we achieved the combined SEDs for 2790 galaxies and 3651 stars detected by BATC and SDSS photometry, including the flux-calibrated BATC SEDs in 13 filter bands and the aperture-corrected SDSS SEDs in 5 filter bands. This SED catalog can be electronically provided upon request.

To describe the errors of BATC magnitudes, we separated all the objects into several sub-groups with magnitude interval of 0.5 mag, and the mean measurement errors at specified magnitudes were derived. We found that the measurement error for each filter band tends to be larger at fainter depth. Except for the n , o and p magnitudes, the errors are about 0.02 for bright stars (say, $m < 16.5$), and less than 0.05 at $m = 19.0$. The measurement errors in n , o and p magnitudes are found to be larger just because of the low sensitivity of our CCD detector in redder filter bands.

4. ANALYSES OF 254 GALAXIES WITH KNOWN SPECTROSCOPIC REDSHIFTS

4.1. Velocity Distribution and SED Catalog

Burns et al. (1995) studied the distribution of measured galaxy velocities for Abell 2255 by using the *ROSTAT* software. Two resistant and robust estimators analogous to the velocity mean and standard deviation, namely the biweight location (C_{BI}) and scale (S_{BI}), are defined to characterize the shape of the velocity distribution (Beers et al. 1990). Burns et al. (1995) found $C_{BI} = 24330^{+203}_{-265}$ km s $^{-1}$ and $S_{BI} = 1240^{+203}_{-129}$ km s $^{-1}$ with only 39 member galaxies. We have 254 galaxies with known spectroscopic redshifts within our field. The distribution of spectroscopic redshifts for all these known galaxies is shown in panel (a) of Fig. 4. There are 214 galaxies occurring in the redshift range of 21,000 km s $^{-1} < cz < 29,000$ km s $^{-1}$, with a sharp peak at $\sim 24,800$ km s $^{-1}$. We also calculated the biweight location and scale for these 214 galaxies using the ROSTAT software, and achieved $C_{BI} = 24025 \pm 89$ and $S_{BI} = 1315 \pm 86$ in km s $^{-1}$. Compared with the results in Burns et al. (1995), the biweight location is smaller and the biweight scale becomes larger with smaller uncertainties. We fitted the velocity distribution in Fig. 4b with single Gaussian, but the Kolmogorov-Smirnov test and Shapiro-Wilk W-test reject a Gaussian distribution at more than 99% confidence level.

We tried to detect and quantify the presence of bimodality in velocity distribution with the KMM algorithm code (Ashman, Bird & Zepf 1994). Two equal-variance Gaussian components with velocity mean values of 23942 and 27454 km s⁻¹ were found to have a good fit with a mixing proportion of 94.2%:5.8%. The KMM algorithm also allows partitioning of data into individual groups. Only 12 (5.8%) cluster galaxies belong to the Gaussian component centered at 27454 km s⁻¹, and they are scattered in this field. The confidence level of rejecting the single Gaussian model is nearly 100%. The significant deviation from single Gaussian distribution and unusually large velocity dispersion might reflect some clues of an unrelaxed system.

Fig. 4: Radial velocity distribution for 214 member galaxies

Table 2 presents the combined SEDs of 254 galaxies with known spectroscopic redshifts, which is structured as follows:

- Column 1: Number of the galaxies (sorted by the distance to cluster center);
- Column 2: R.A. in 2000 epoch, in “hhmmss.s” mode, given by NED;
- Column 3: Declination in 2000 epoch, in “ddmmss” mode, given by NED;
- Column 4: Spectroscopic redshift, given by NED;
- Column 5: Photometric redshift, estimated by the combined SED;
- Column 6 - 18: Photometric magnitudes in 13 BATC filter bands. The value of 0.0 means out of field;
- Column 19 - 23: Aperture-corrected photometric magnitudes in five SDSS filter bands.

It should be noted that the photometric magnitudes given in Table 2 might be somewhat different from the magnitudes given in the literature. What we attempt to obtain is the *relative* SEDs within a fixed aperture for the galaxies in the region of Abell 2255.

Table 2: Combined SEDs of 254 known galaxies

4.2. Spatial Distribution and Localized Velocity Structure

Fig. 5a presents the spatial distribution of 214 known member galaxies within our field of view, including 168 (88%) early-type galaxies and 46 (12%) late-type galaxies, with respect to the NED-given central position of Abell 2255, R.A.= $17^h12^m31^s$ and Decl.= $64^\circ05'33''$ (for the J2000 equinox). Early- and late-type galaxies are denoted by open circles and crosses, respectively. It can easily be seen that the early-type galaxies dominate in the central region. We superpose the contour map of the surface density which has been smoothed by a Gaussian window with $\sigma = 2$ arcmin. The spatial distribution of 214 bright member galaxies seems to deviate from spherically symmetric. The contours of surface density are elongated in an east-west direction in the central region. The isophotes are offset from the positions of two cD galaxies (marked as “+”), but seem to have a centroid located between the cD galaxies and the X-ray emission centroid (R.A.= $17^h12^m45^s$ and Decl.= $64^\circ03'54''$, mark as “×”) derived by the ROSAT imaging observations (Feretti et al. 1997). The contours show that there might be five satellite clumps (i.e., subclusters) of galaxies whose surface densities are more than 0.15 galaxies

arcmin^{-2} (namely A, B, C, D, and E) surrounding the main concentration. The contour curves at 0.15 galaxies arcmin^{-2} can be used to define the clump areas.

However, these clumps might be enhancements simply due to projection effects. The proper way to find out the true substructures is to observe how significant is the localized variation at clumps' positions in the line-of-sight velocity distribution. Dressler & Shectman (1988) designed a statistical test, so-called Δ -test, for computing the deviation of local velocity mean and dispersion from those of the overall velocity distribution. In the spirit of Δ -test, Colless & Dunn (1996) developed a new test (so-called κ -test) for quantifying localized variation in velocity distribution, by defining a new test statistic κ_n to characterize the local deviation on the scale of groups of n nearest neighbors. The larger κ_n , the greater the possibility that the local velocity distribution differs from the overall distribution. The probability that κ_n is larger than the observed value κ_n^{obs} , $P(\kappa_n > \kappa_n^{\text{obs}})$, can be estimated by Monte Carlo simulations by randomly shuffling velocities. Table 3 gives the results of κ -test for 214 known member galaxies, and the number of simulations is 10^3 for all cases.

Table 3: Result of κ -Test for 214 Member Galaxies

n	5	6	7	8	9	12	15	20
$P(\kappa_n > \kappa_n^{\text{obs}})$	0.003	0.002	0.003	0.006	0.007	0.005	0.005	0.023

The presence of substructures in Abell 2255 is strongly supported by the local velocity variation with a wide range of neighbor sizes. The six nearest neighbors is the optimum scale on which substructure is most obvious. The bubble plot in Fig. 5b shows the location of localized variation using neighbor size $n = 6$, and the bubble size for each galaxy is proportional to $-\log[P_{KS}(D > D_{\text{obs}})]$. Therefore larger bubbles indicate a greater difference between local and overall velocity distributions. A close comparison between two panels in Fig. 5 shows that the bubble clustering appears at the positions of clumps A, B and C. The clumps D and E seems to be unreal substructures in the line-of-sight velocity distribution. The dynamics for substructures A, B and C will be discussed in §6.

Fig. 5: (a) Spatial distribution for 214 galaxies; (b) Bubble plot

4.3. Color-Magnitude Correlation

A correlation between color and absolute magnitude for early-type galaxies, the so-called C-M correlation, has been found for some rich galaxy clusters (see Bower et al. 1992, and references therein). For the early-type galaxies in a cluster, the fainter galaxies tend to have colors bluer than the brighter galaxies do. The measured magnitudes in BATC and SDSS photometries for the galaxies in Abell 2255 can be directly used to demonstrate the C-M correlation.

Fig. 6 gives plots of two color indices (C.I.'s), $u' - p$ and $u' - o$, versus magnitude in the h bandpass for 214 known member galaxies in Abell 2255. The galaxies with different morphological types are denoted by different symbols. A very clear C-M correlation can be found for 137 elliptical

galaxies, in the sense that the brighter galaxies are redder. We have following linear fits by method of least squares:

$$u' - p = -0.136(\pm 0.04)h + 5.758(\pm 0.669),$$

$$u' - o = -0.134(\pm 0.04)h + 5.606(\pm 0.638).$$

The linear fits are plotted as solid lines, and the dashed lines in panels (a) and (b) represent $\sigma_{C.I.} = 0.669$ and 0.638 , respectively. More than 95% elliptical galaxies are distributed between the dashed lines. The linear relations are quite similar to those we found for bright galaxies in Abell 2634 (Yuan et al. 2001). It is evident that spiral galaxies do not obey such a correlation, and lenticular galaxies behave as something between the ellipticals and the spirals in the C-M relation. Based on the significantly different behavior for galaxies with different morphologic types, the C-M diagram can be used to distinguish early- and late-type galaxies (e.g., Colless & Dunn 1996).

Fig. 6: Color-magnitude diagram for 214 known member galaxies

4.4. Application of the Photometric Redshift Technique

The technique of photometric redshift can be used to estimate the redshifts of galaxies with the combined SED information. For a given object, the photometric redshift, z_{phot} , corresponds to the best fit (in the χ^2 -sense) of its photometric SED by the set of template spectra. Based on the standard SED-fitting code called HYPERZ (Bolzonella, Miralles, & Pelló 2000), the procedures for estimating the photometric redshifts have been developed especially for the BATC multicolor photometric system (Xia et al. 2002). This technique is traditionally used to search for galaxies or AGNs with comparatively high redshifts. Thanks to the large number of filters (13 BATC bands plus 5 SDSS bands), the accuracy of photometric redshift estimates can be expected to be largely improved even for nearby galaxies. The sample of 254 galaxies with known spectroscopic redshifts allows an opportunity to check whether the method of SED combination for the SDSS and BATC surveys can lead to a more accurate z_{phot} estimate for the nearby galaxies with $z < 0.5$.

Fig. 7 shows the plot of photometric redshift (z_{phot}) versus spectroscopic redshift (z_{sp}) for 254 galaxies, including the member galaxies and background galaxies. In our calculations, only the normal galaxies were taken into account in the reference templates, and the reddening law with a $A_V \sim 0.3$ by Calzetti et al. (2000) was adopted. The photometric redshift for each known galaxy was searched within a redshift range from 0.0 to 1.0, with a searching step of 0.01. The dotted line in Fig. 7 corresponds to $z_{phot} = z_{sp}$, and the error bar in the z_{phot} determination at 68% confidence level is also given. It can easily be seen that our z_{phot} estimate is basically consistent with the spectroscopic redshift: more than 90% member galaxies in Abell 2255 are found to have $z_{phot} \sim 0.075 \pm 0.015$, and the background galaxies with $z_{sp} < 0.5$ also scattered along the critical line $z_{phot} = z_{sp}$. Compared with our previous z_{phot} estimate for the nearby galaxies in Abell 2634 ($z \sim 0.03$) on the basis of the BATC SED information only (see Fig. 6 in Yuan et al. 2001), this run of z_{phot} determination has smaller uncertainties and deviations in general. Fig. 8 shows an example for the best fit to

the combined SED of the early-type galaxy SDSS J171236.07+640508.0. The combined SED has a higher spectral resolution, which is crucial for decreasing the uncertainty of z_{phot} estimate. This result demonstrates not only the efficiency of our SED-fitting procedures, but also the reliability of our method of combining the photometric data from the SDSS and BATC photometric observations.

Fig. 7: $z_{sp} - z_{phot}$ for 254 known galaxies

Fig. 8: The best fit of SDSS J171236.07+640508.0

Our method described above opens a straightforward way for obtaining the optical SEDs from the SDSS and BATC multicolor photometries of the faint galaxies. Our investigations on spatial distribution and color-magnitude relation of the galaxies in Abell 2255 can then be extended to an unprecedented depth. It should be noted that the error in the photometric redshift is much larger than the cluster velocity dispersion.

5. SED SELECTION OF FAINT CLUSTER GALAXIES

In total, 6441 objects within our BATC observation field are found to have the counterparts in the SDSS imaging observations, of which 2776 objects are characterized by the SDSS star/galaxy separation pipeline, *frames*, as extended sources (i.e., galaxies). After an exclusion of 254 known galaxies, there remain 2522 galaxies without any redshift information. Based on their combined SEDs, we applied the photometric redshift technique to them, and derived their optimal estimates of z_{phot} values.

Since the error in z_{phot} determination is larger than the intrinsic dispersion (say, biweight scale S_{BI}) in distribution of spectroscopic redshift, the z_{phot} distribution for faint cluster galaxies should peak at ~ 0.08 with a larger dispersion. Fig. 9 shows the z_{phot} distribution for 2522 galaxies. The peak at $z_{phot} \sim 0.08$ should be associated with Abell 2255. Based on the fact that more than 98% known member galaxies are found to have their redshifts within a range of $20,400 \text{ km s}^{-1} < cz < 27,000 \text{ km s}^{-1}$ (see Fig. 4), we conservatively adopt this range as the limits for membership determination. As a result, 328 galaxies having their photometric redshifts between 0.068 and 0.090 are selected to be member candidates.

Fig. 9: The z_{phot} distribution for 2522 galaxies

Among 328 member candidates, 266 (81%) galaxies are regarded as early-type galaxies by our SED-fitting procedures. A further selection by C-M correlation for these early-type galaxies can be performed. We find that the majority of early-type candidates agree with the C-M relation derived by 137 bright early-type galaxies in §4.3. However, there are 48 early-type candidates with colors beyond the 2σ deviation of intercept, and they might have been misclassified. Taking only the templates of late-type galaxies, we performed the photometric redshift estimate again for these 48 candidates, and

15 candidates are found to have photometric redshifts beyond the range of $0.068 < z_{phot} < 0.090$. They are therefore regarded as non-member galaxies, and the remaining 33 galaxies are regarded as late-type member galaxies.

Finally, 313 faint galaxies (including 218 early-types and 95 late-types) are selected as faint member galaxies in Abell 2255. Table 4 presents the catalog of SED information for these new members, as well as SDSS-measured position, z_{phot} value, and morphological class T (E, S0, Sa, Sb, Sc, Sd, and Im galaxies are represented by 1 to 7, respectively).

Table 4: SED Catalog of 313 galaxies

6. ANALYSES OF THE ENLARGED SAMPLE OF CLUSTER GALAXIES

6.1. Velocity Distributions and Substructures

Some interesting and unusual characteristics in radio, and X-ray bands support a picture that Abell 2255 may be in the process of merging with a galaxy cluster/group (Feretti et al. 1997). Fig. 10 shows the redshift distributions for (i) 203 galaxies in a central region with a radius of 10 arcmin, (ii) 406 early-type galaxies, (iii) 121 late-type galaxies, and (iv) 527 cluster galaxies in the enlarged sample. Since two peaks, respectively, at 24900 and 23700 km s $^{-1}$ can be found in subset (i),(ii) and the total sample, we assumed two homoscedastic Gaussian components in the KMM algorithm code to search for bimodality in above velocity distributions. However, none of these tests indicate that a bimodal distribution is a statistically significant improvement over the single Gaussian. Compared with the velocity distribution of 214 known galaxies in Fig.4b, the enlarged sample has a larger biweight scale (1848 km s $^{-1}$). This should be due to the large error in photometric redshift estimate for 313 newly-selected member galaxies, and it will probably smooth the bimodality detected in Fig. 4b.

Fig. 10: Velocity distributions for four samples
--

The vast majority of 313 newly-selected member galaxies are fainter than $h \sim 17.6$, and the early-type faint galaxies dominate in the central 10-arcmin region. Compared with the sample of 214 known cluster galaxies, these faint galaxies have a higher fraction of late-type galaxies (30%), and most of late-type galaxies are scattered around the main concentration. The spatial distribution of the enlarged sample of 527 cluster galaxies is shown Fig. 11a. In general the contour map of this rich cluster appears to be elongated along southwest and northwest directions. The cluster centroid seems to agree well with that shown in Fig.5a.

Fig. 11: (a) Spatial distribution of 517 galaxies; (b) Bubble plot
--

To observe the substructures in the velocity distribution, we applied the κ -test on the enlarged sample of cluster galaxies. The κ -test results for 10^3 simulations are given in Table 5. For the cases with neighbor size of $n \leq 8$, the substructures are still significant with the probabilities $P(\kappa_n > \kappa_n^{obs}) < 10\%$. The degree of difference between the local velocity distribution for groups of six nearest neighbors and

the overall velocity distribution is shown by the bubble plot in Fig. 11b. Compared with Fig. 5b, substructure A becomes less conspicuous, and substructures B and C remain with similar significance. Additionally, no clustering of large bubbles are found at the positions of clumps D and E in Fig. 11b, indicating that clumps D and E may not be real substructures in velocity distribution.

Within the areas of clumps A, B and C, defined by the contour curve at 0.15 arcmin^{-2} in Fig. 5a, there are 10, 17 and 8 galaxies, respectively. Table 6 shows the statistics of line-of-sight velocity distributions for these galaxies. Because of the small number of galaxies in the substructures, we used the ROSTAT software to compute the biweight locations and scales. It is interesting to find that subclusters A and C locate at the opposite sides of the central concentration, and they are likely to have reverse distribution of peculiar velocities, respective to the systemic redshift of 0.0806. If we regard the biweight location of the velocity distribution of 214 known member galaxies ($C_{BI} = 24025 \pm 89$) as systemic receding velocity, subcluster A tends to move toward us at more than 99% confidence level, and subcluster C tends to depart from us at nearly 2σ significance. Additionally substructure B has a slight tendency similar to substructure C. This might be a direct evidence for an unrelaxed system, and supports a recent merge event. We applied the same statistics to the spectroscopically confirmed galaxies in these three substructures, and similar dynamical picture was achieved. This should be the first report of the direct dynamical evidence in optical band for an on-going merger in Abell 2255.

Table 5: Result of κ -Test for 527 Cluster Galaxies

n	5	6	7	8	9	12	15	20
$P(\kappa_n > \kappa_n^{obs})$	0.026	0.017	0.057	0.097	0.133	0.174	0.184	0.223

Table 6: Properties of Substructures A, B, and C

Statistic	Substructure A	Substructure B	Substructure C
Size (known+new)	6+4	10+7	7+1
Galaxy No. in Table 2	116,123,126,133, 134,148	118,129,130,137,140, 142,152,153,162,167	138,154,166,169 172,173,178
Galaxy No. in Table 4	266,268,269,271	41,42,44,61,62,63,72	27
Mean Velocity (km s^{-1})	23190 ± 528	24408 ± 448	24711 ± 415
Standard Deviation (km s^{-1})	1668	1848	1173
Biweight Location (km s^{-1})	23109 ± 257	24400 ± 482	24893 ± 459
Biweight Scale (km s^{-1})	748 ± 599	1908 ± 220	1144 ± 542

6.2. Color Properties and Luminosity Function

The C-M relations for the enlarged sample are shown in Fig. 12, spanning a wider range of the h magnitude from 15.0 to 20.5. The SDSS spectroscopic target selection of the main galaxy

sample is complete to $r' < 17.77$ (Strauss et al. 2002), which has been well shown in Fig. 12. The linear relationship defined by the bright known early-type galaxies can well be extended to the faint early-type galaxies. This correlation can be understood by the fact that the reddening of galaxies is mainly caused by the rich metal absorption in stellar spectra shortward of 4250 Å, and it tends to be more significant for bright early-type galaxies. Such a correlation was also found for the early-type galaxies in Virgo and Coma clusters, and elliptical galaxies seem to have a tighter correlation than the lenticular galaxies do (Bower et al. 1992). Furthermore, the late-type galaxies have a larger dispersion of color indices than the early-types (Yuan, et al. 2001).

Fig. 12: The C-M relations for all cluster galaxies

The luminosity function (LF) in a cluster is a powerful and fundamental means to study galaxy formation and evolution in a dense environment. Recent studies showed that the LF for cluster galaxies differ from one cluster to another, and even from one region to another region in one cluster (Biviano et al. 1995; Durret et al. 2002). Our photometry for all member galaxies in Abell 2255 provide a good sample for studying the LF for the bright galaxies in a rich cluster. Some previous studies on nearby rich clusters show that there may be at least two components in the galaxy LF, a Gaussian distribution for the bright galaxies and another component for fainter cluster galaxies formulated by the Schechter function or a power law (Durret et al. 1999). For comparison with other investigations, we have chosen to plot the LF in traditional R - and V -band magnitudes which can be calculated by $R = i + 0.1036(\pm 0.055)$ and $V = g + 0.3292(f - h) + 0.0476(\pm 0.027)$ (Zhou, et al. 2003). Fig. 13 shows the distribution of R and V magnitudes for all galaxies in Abell 2255. The LFs are significantly asymmetric, with a peak at $R \sim 17.5$ and $V \sim 17.7$ respectively. The vast majority of bright member galaxies ($R < 17.5$ or $V < 17.8$) has been confirmed by the SDSS spectroscopies. It is clear that these previously known data-set may not strongly constrain the LF shape because the peak of LF can not be well determined.

The application of the photometric redshift technique to 254 known galaxies shows that the selection criterion $0.068 < z_{phot} < 0.090$ excludes nearly 10% of the true members, and leads to about 5% contamination by background galaxies. The success rate for membership selection based on our SED-fitting procedures should be still over 80% for the bright galaxies. Though the uncertainty in membership selection might be larger for faint galaxies, the LF peak shown in Fig. 13 should be real because the BATC photometry are complete for the galaxies brighter than 19.0 mag in all filter bands (see Table 1). The magnitude distribution for the cluster galaxies brighter than 19.0 mag can be expected to put a strong constraint on the true LF shape. Therefore we used the minimum χ^2 method to fit the bright part of the differential LF with (i) a Schechter function: $S(m) = K_S 10^{0.4(m^*-m)(\alpha+1)} \exp[-10^{0.4(m^*-m)}]$, and (ii) a Gaussian function: $G(m) = K_G \exp[-(m - \mu_m)^2/(2\sigma_m^2)]$. The best fit parameters are also shown in Fig. 13.

The accuracy of z_{phot} estimate is comparatively high for the brighter galaxies that have smaller magnitude errors, so the bright member galaxies have higher possibility to be selected. The bright part of the LF can be fitted well with a single Gaussian defined by a central absolute magnitude

of $\mu_{M_V} = -20.3(\pm 0.1)$ and a dispersion of $\sigma \sim 1.02(\pm 0.09)$, which is consistent with the Gaussian component for Coma LF, $\mu_{M_V} = -20.4(\pm 0.2)$ and $\sigma = 1.1(\pm 0.3)$ (Lobo, et al. 1997). A better fit to the faint part of the LF can be obtained using a single Schechter function with $M_V^* = -20.58(\pm 0.25)$ and $\alpha = -0.136(\pm 0.275)$, though there exists an excess in the bright end of LFs. The LF curve for the cluster galaxies fainter than 19.0 mag has a significant excess above the Gaussian fitting, and another component of a Schechter function seems to be needed to give a better fit to the faint part. However, our sample for dwarf cluster galaxies is far from complete because a large number of faint galaxies can not be detected by the BATC multicolor system. The lack of BATC SED information prevents an accurate membership selection for dwarf galaxies in Abell 2255.

Fig. 13: Distributions of $R-$ and $V-$ magnitudes

7. SUMMARY

This paper presents our multicolor optical photometry for the nearby rich cluster of galaxies Abell 2255, using the 60/90 cm Schmidt Telescope of the BAO equipped with 13 BATC filters that cover almost whole optical wavelength domain. A method of SED combination for the SDSS and BATC photometries has been explored. After an aperture correction of the SDSS *model* magnitudes and a flux calibration of the BATC magnitudes, the SEDs obtained by these two photometric systems were carefully combined. A sample of 254 galaxies with known spectroscopic redshifts in the region of Abell 2255 was then formed for verifying the reliability of the combined SEDs. We applied the technique of photometric redshift upon this sample, and more than 90% of the member galaxies are found to have photometric redshifts between 0.068 and 0.090, which provides a reliable tool for further membership selection. This results showed that the combined SEDs with higher resolution could lead to a more accurate estimate of photometric redshift. We selected 214 known member galaxies from our SED lists, for which the detailed analyses on their spatial and color properties are performed. We found that the core region of Abell 2255 is populated by early-type galaxies, and the late-type galaxies are scattered. 137 known early-type galaxies are found to have a tight color-magnitude correlation.

The cross-identification of the SDSS-listed extended sources with our SED list yields a large sample which contains 2522 faint galaxies without redshift information. Based on the knowledge of SED features for known cluster galaxies, we performed our SED-fitting procedures for estimating the photometric redshifts for these faint galaxies. The color-magnitude correlation was also used to constrain our membership selection. As a result, we isolated 313 galaxies as the faint members. The C-M relation for this enlarged sample of cluster galaxies shows that the tight correlation defined by bright galaxies can be extended to the faint early-type galaxies, and the late-type galaxies have a larger dispersion of color index. Our sample of 527 cluster galaxies is nearly complete up to $V = 19.0$, one magnitude fainter than the LF maximum, which could put a strong constraint on the LF shape. Subclusters A and C located on opposite sides of the cluster center are found to have reverse tendencies in their peculiar velocities, which obviously supports the picture of cluster/group merger in this cluster,

as proposed by the radio and X-ray observations.

It should be noted that the combined SED measures through a fixed aperture offers a higher spectral resolution for all the objects detected in the BATC and SDSS surveys, which will surely benefit each other. Our candidate list of faint member galaxies provides the targets for follow-up SDSS spectroscopic observations. For a further investigation on dynamics and luminosity function of galaxies in such a rich cluster possessing an on-going cluster/group merger, the deep spectroscopic observations for the sake of obtaining the accurate redshifts for the faint member galaxies is necessary.

We acknowledge the anonymous referee for his thorough reading of this paper and invaluable suggestions. We are grateful to Dr. Beers, R. C. and Ashman, K. M. for their kindly providing the ROSTAT software and the KMM algorithm code which has been used in this work. We have made use of the NASA/IPAC Extragalactic Database (NED) which is operated by the Jet Propulsion Laboratory, California Institute of Technology, under contract with the National Aeronautics and Space Administration. This work is mainly supported by the National Key Base Sciences Research Foundation under the contract TG1999075402 and is also supported by the Chinese National Science Foundation (NSF) under the contract No.10273007. We would like to thank Prof. Jiansheng Chen, Dr. Jun Ma, Hong Wu and Yanbin Yang for their helpful discussions, and Prof. Helmut Abt for his help in improving the English. We also appreciate the assistants who contributed their hard work to the observations.

REFERENCES

- Abell, G. O. 1958, ApJS, 3, 211
Ashman, K. M., Bird, C. M., & Zepf, S. E. 1994, AJ, 108, 2348
Bautz, L., & Morgan, W. 1970, ApJ, 162, L149
Beers, T. C., Flynn, K., & Gebhardt, K. 1990, AJ, 100, 32
Bird, C. M. 1994, AJ, 107, 1637
Biviano, A., Durret, F., Gerbal, D. et al. 1995, A&A, 297, 610
Bolzonella, M., Miralles, J. -M., & Pelló, R. 2000, A&A, 363, 476
Bower, R. G., Lucey, J. R., & Ellis, R. S. 1992, MNRAS, 254, 589
Burns, J. O., Roettiger, K., Pinkney, J., et al. 1995, ApJ, 446, 585
Calzetti, D., Armus, L., Bohlin, R. C., et al. 2000, ApJ, 533, 682
Capaccioli, M., Held, E. V., Lorenz, H., & Vietri, M. 1990, AJ, 99, 1813

- Colless, M., & Dunn, A. M. 1996, ApJ, 458, 435
- Davis, S. D., & White, R. E. 1998, ApJ, 492, 57
- de Vaucouleurs, G. 1948, Annales d'Astrophysique, 11, 247
- de Vaucouleurs, G., & Capaccioli, M. 1979, ApJS, 40, 699
- Dressler, A., & Shectman, S. 1988, AJ, 95, 985
- Durret, F., Gerbal D., Lobo C., & Pichon C. 1999, A&A, 343, 760
- Durret, F., Adami, C., & Lobo, C. 2002, A&A, 393, 439
- Fan, X., Burstein, D., Chen, J., et al. 1996, AJ, 112, 628
- Feretti, L., Böhringer, H., Giovannini, G., and Neumann, D. 1997, A&A, 317, 432
- Ferguson, H., Dickinson, M., Williams, R. E. 2000, ARA&A, 38, 667
- Fukugita, M., Ichikawa, T., Gunn, J. E., Doi, M., Shimasaku, K., & Schneider, D. P. 1996, AJ, 111, 1748
- Lobo, C., Biviano, A., & Durret, F., et al. 1997, A&A, 317, 385
- Lupton, R. H., Gunn, J. E., Ivezić, Z., et al. 2001, in ASP Conf. Ser. 238, Astronomical Data Analysis Software and Systems X, ed. F. R. Harnden, Jr., F. A. Primini, & H. E. Payne (San Francisco: ASP), 269
- Stauffer, J., Spinrad, H., & Sargent, W. L. W. 1979, ApJ, 228, 379
- Strauss, M. A. et al. 2002, AJ, 124, 1810
- Stoughton, C., Lupton, R. H., Bernardi, M., et al. 2002, AJ, 123, 485
- Struble, M. F., & Rood, H. J. 1982, AJ, 87, 7
- Struble, M. F., & Rood, H. J. 1999, ApJS, 125, 35
- Tribble, P. C. 1993, MNRAS, 263, 31
- Williams, R. E., Blacker, B., Dickinson, M., et al. 1996, AJ, 112, 1335
- Xia, L., Zhou, X., Ma, J., et al. 2002, PASP, 114, 1349
- Yan, H., Burstein, D., Fan, X. et al. 2000, PASP, 112, 691
- York, D. G., Adelman, J., Anderson, J. E., et al. 2000, AJ, 120, 1579
- Yuan, Q., Zhou, X., Chen, J., et al. 2001, AJ, 122, 1718

- Zabludoff, A. I., Huchra, J. P., Geller, M. J., 1990, ApJS, 74, 1
- Zehavi, I., Blanton, M. R., Frieman, J. A., et al. 2002, ApJ, 571, 172
- Zhou, X., Chen, J., Xu, W., et al. 1999, PASP, 111, 909
- Zhou, X., et al. 2001, ChJAA, 1, 372
- Zhou, X., Jiang Z., Ma, J., et al. 2003, A&A(accepted) (astro-ph/0209459)

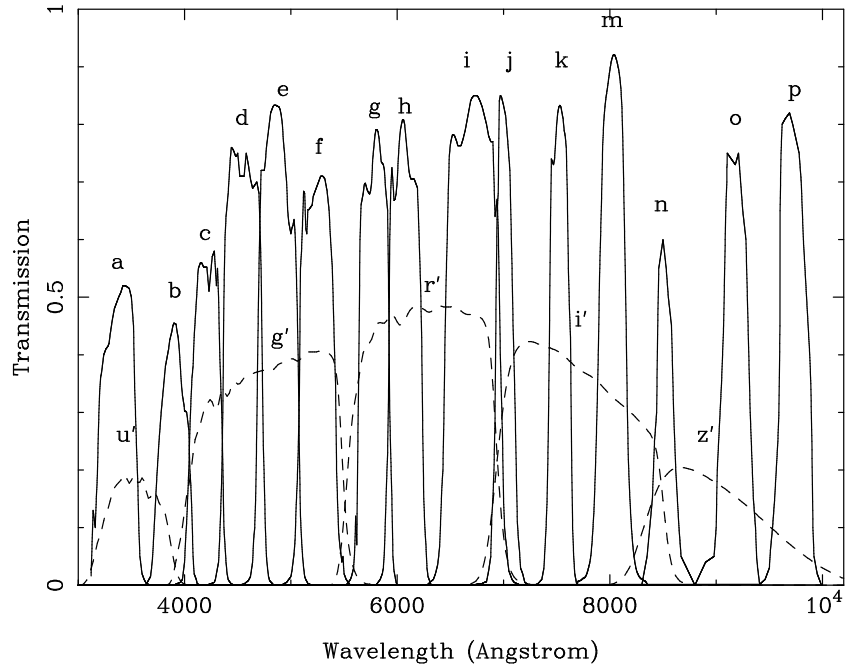


Fig. 1.— The transmission curves of the BATC and SDSS filters. The name of each filter is labelled on the top of transmission curve.

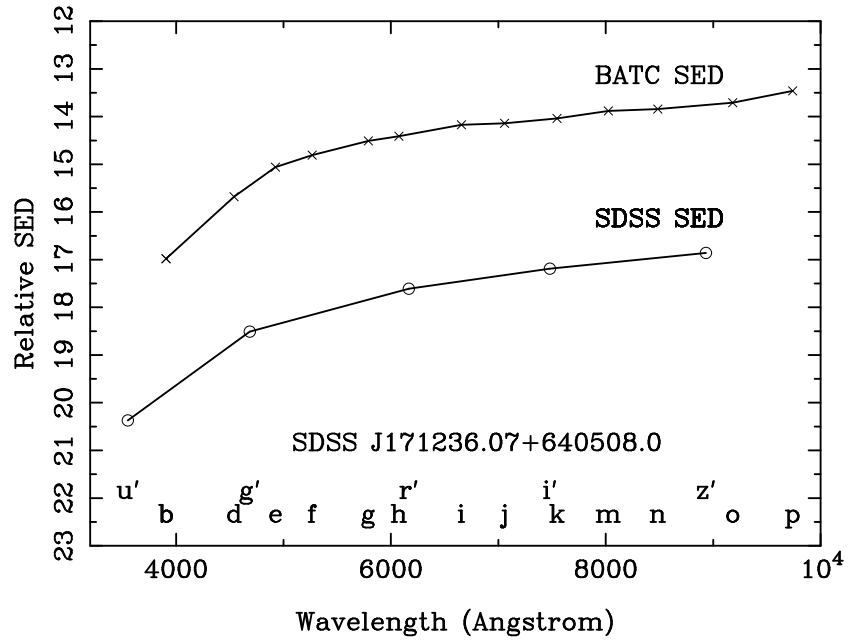


Fig. 2.— The relative SEDs in the BATC and SDSS multicolor systems for the source SDSS J171236.07+640508.0, the central early-type galaxy in Abell 2255 cluster.

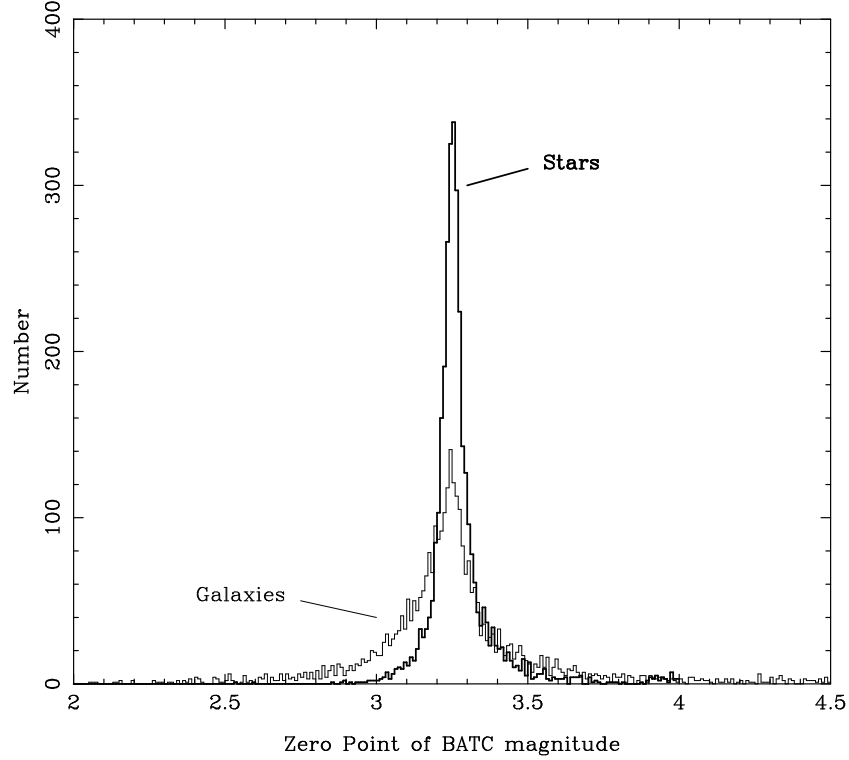


Fig. 3.— Distribution of the zero-points for the stars and galaxies detected by both multicolor surveys.

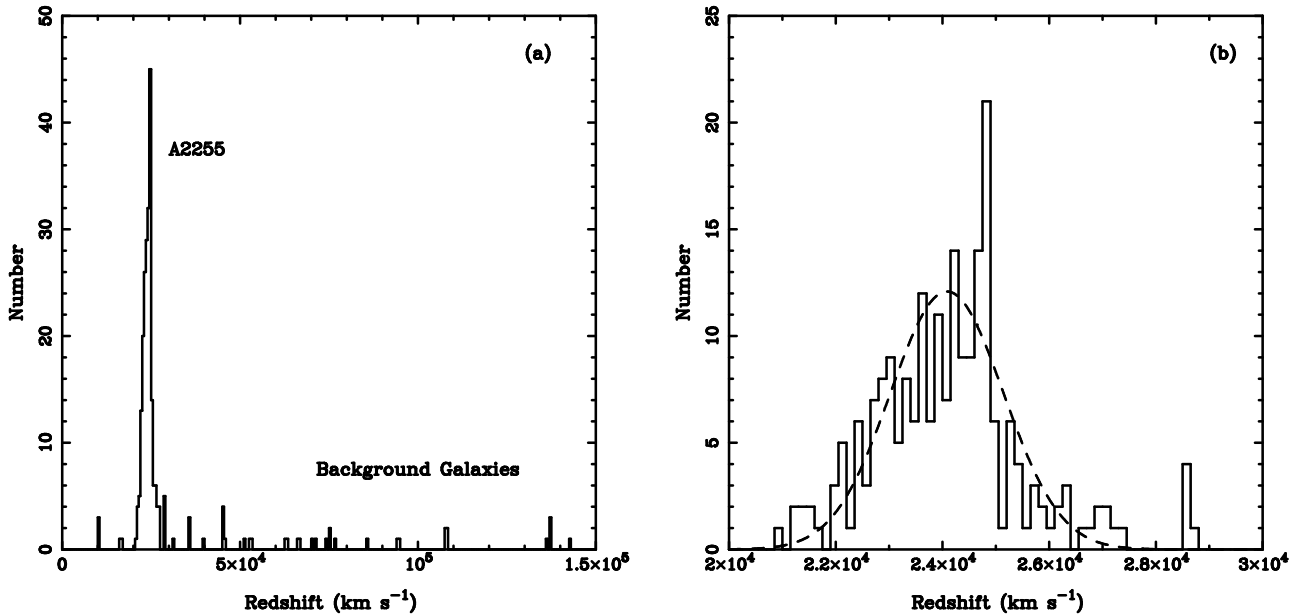


Fig. 4.— Distribution of spectroscopic redshifts for (a) 254 known galaxies and (b) 214 member galaxies. The bin widths are 500 and 150 km s⁻¹, respectively. The best-fitting Gaussian model is also shown in panel (b).

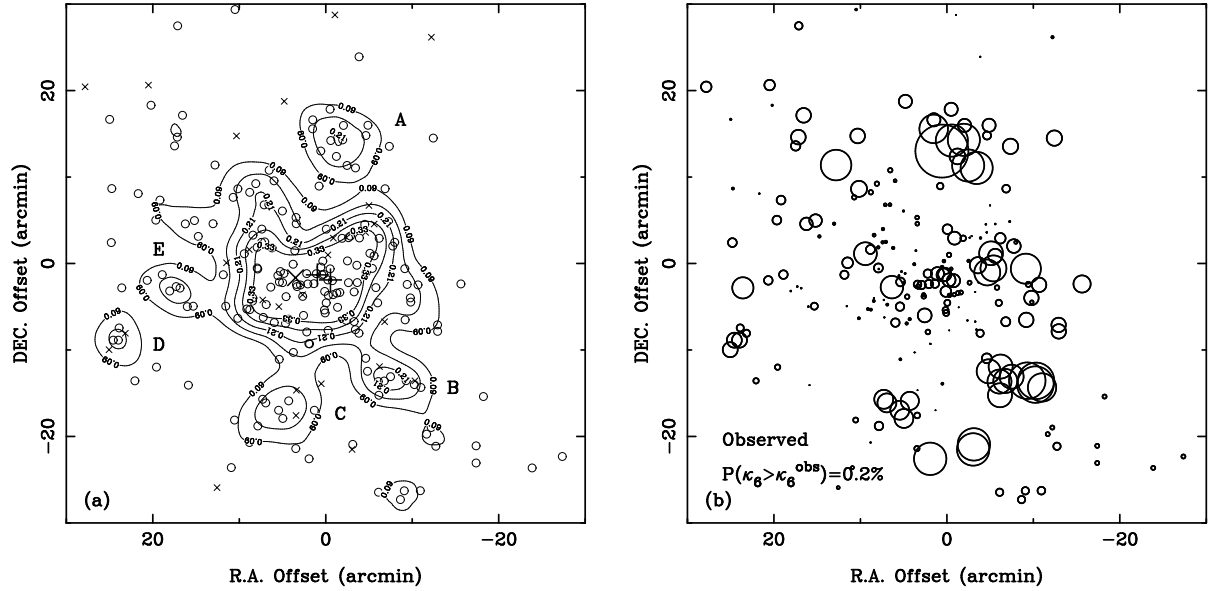


Fig. 5.— (a) Spatial distribution of 214 member galaxies, including 168 early-type galaxies (*open circles*) and 46 late-type galaxies (*crosses*). The contour map of the surface density for all these galaxies using the smoothing window with a radius of 2 arcmin is also given. The contour levels are 0.09, 0.15, 0.21, 0.27 and 0.33 arcmin⁻², respectively. The positions for two central cD galaxies, ZwCl 1710.4+6401 A and B, are flagged as “+”, and the center of X-ray emission is flagged as “×”. The contour curves at 0.15 galaxies arcmin⁻² are used to define the clump areas. (b) Bubble plot showing the localized variation for groups of six nearest neighbors.

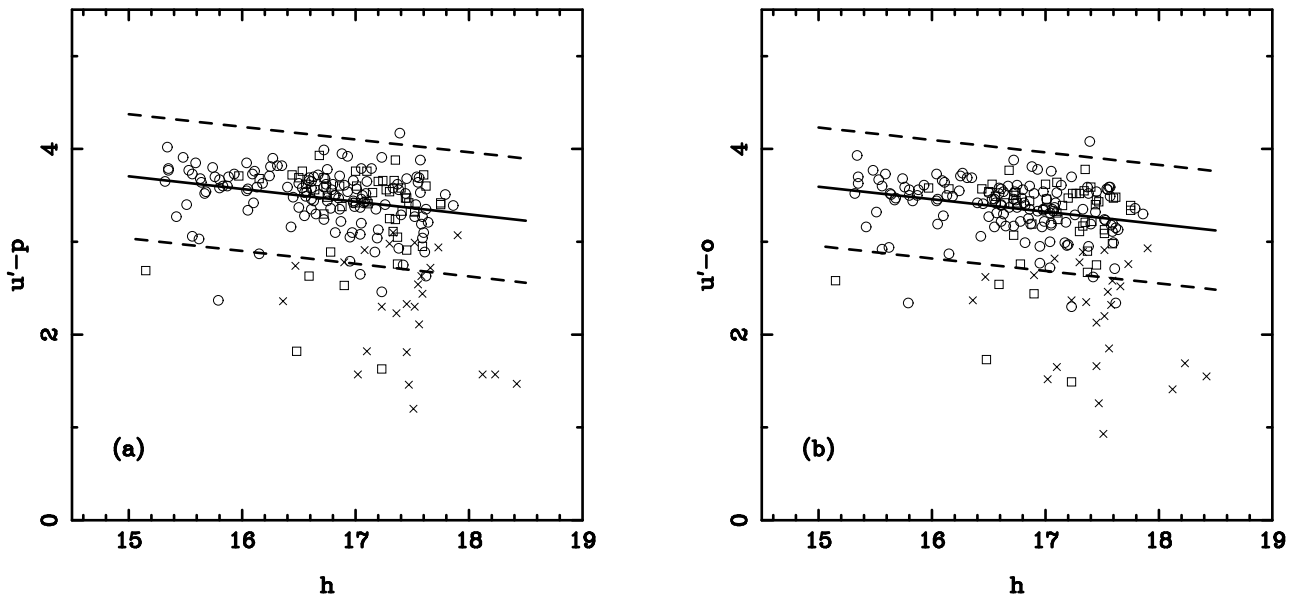


Fig. 6.— Color-magnitude relation for known galaxies in Abell 2255, i.e., the plot of color indices $u' - p$ and $u' - o$ versus h magnitude for 137 elliptical galaxies (*open circles*), 51 lenticular galaxies (*open squares*), and 26 spiral galaxies (*crosses*).

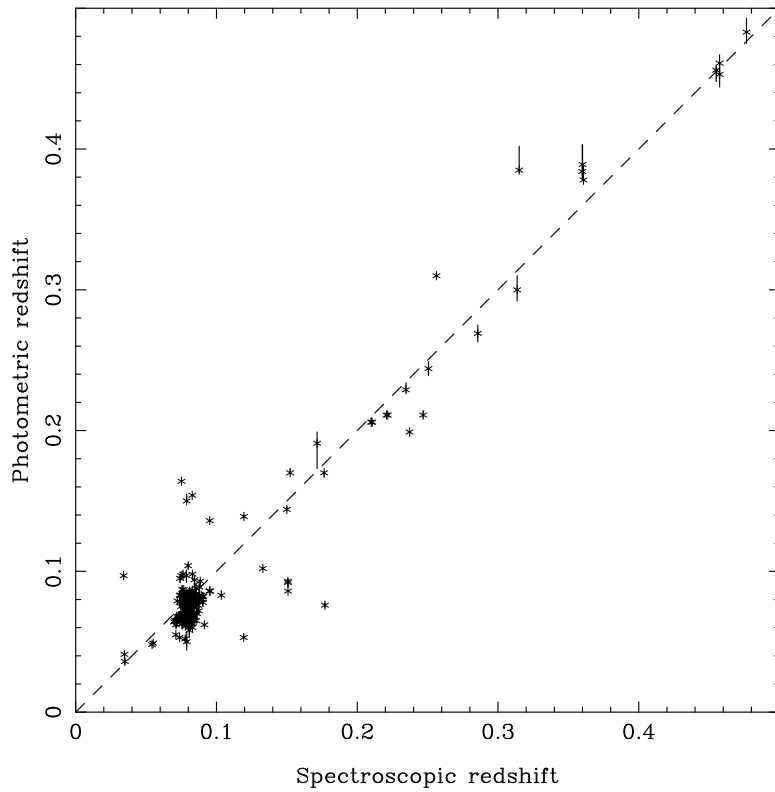


Fig. 7.— Comparison between the photometric redshift (z_{phot}) and spectroscopic redshift (z_{sp}) for 254 galaxies with known spectroscopic redshifts in the region of Abell 2255.

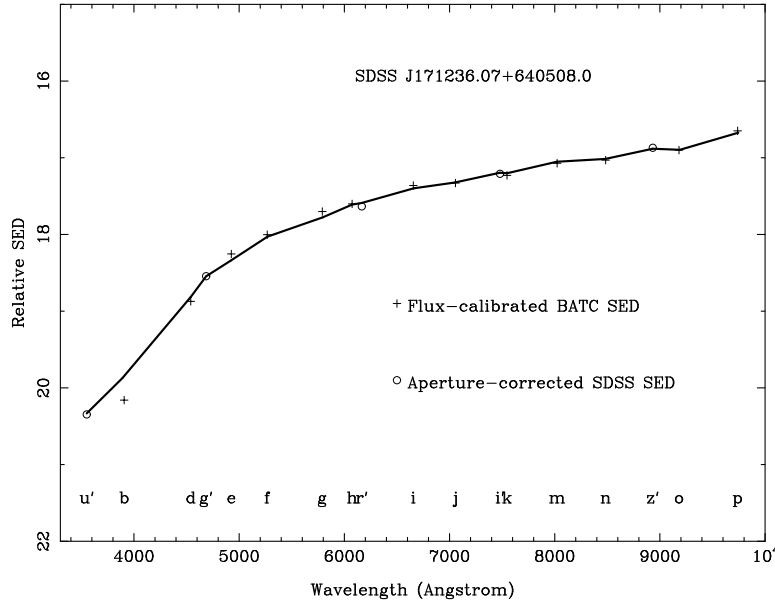


Fig. 8.— The best fit of the combined SED of the source SDSS J171236.07+640508.0, the central early-type galaxy in Abell 2255 cluster

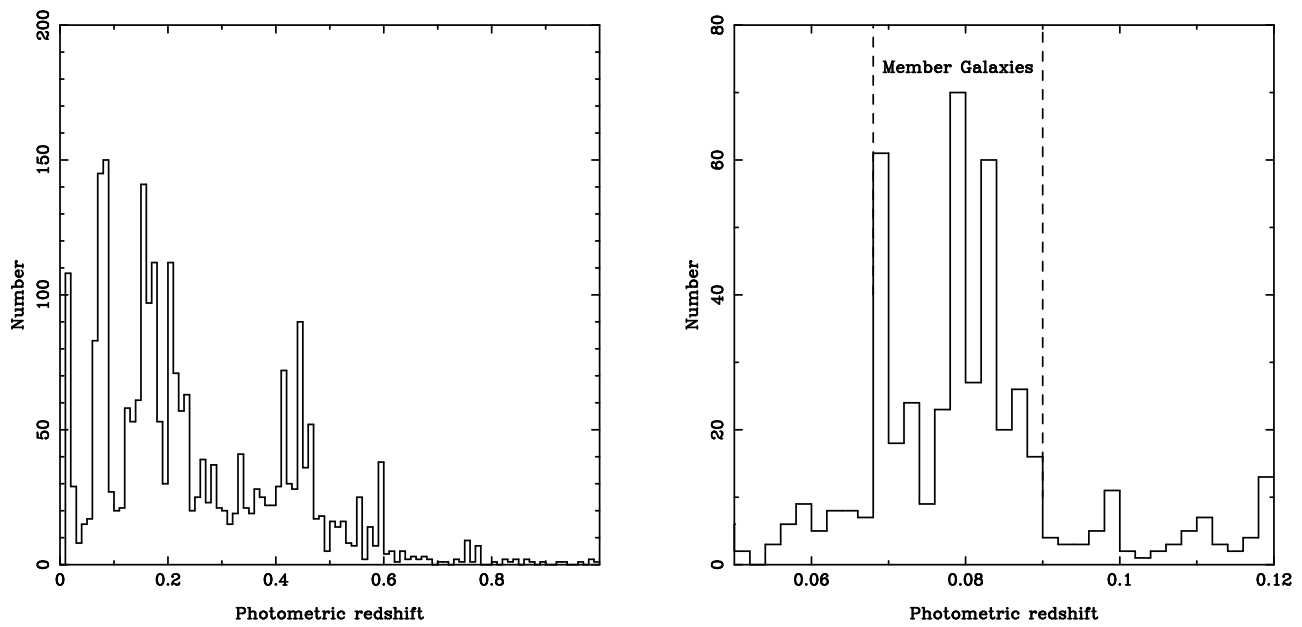


Fig. 9.— Distribution of estimated photometric redshifts for 2522 faint galaxies

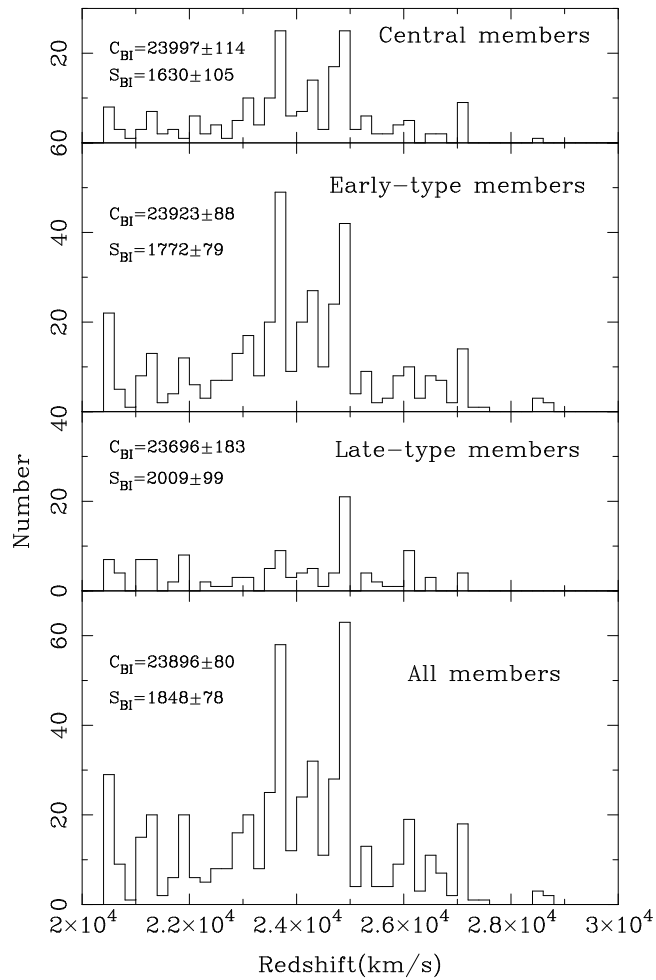


Fig. 10.— Redshift distributions for (i) 203 galaxies in central region with a radius of 10 arcmin, (ii) 406 early-type galaxies, (iii) 121 late-type galaxies, and (iv) the total sample of 527 cluster galaxies.

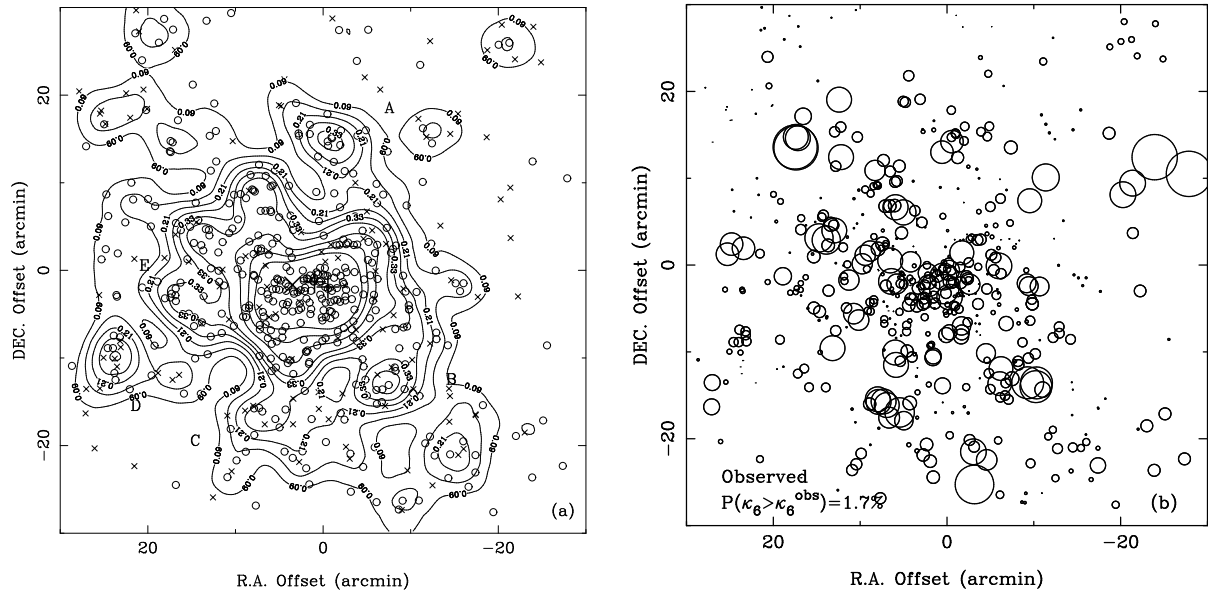


Fig. 11.— (a) Spatial distributions for all member galaxies. Early-type galaxies are denoted by open circles, and the late-type galaxies by crosses. The contour maps of the surface density are also superposed. The contour levels are 0.09, 0.15, 0.21, 0.27, 0.33, 0.39, 0.51, 0.63, and 0.75 arcmin⁻². The positions for two central cD galaxies, ZwCl 1710.4+6401 A and B, are flagged as ‘+’, and the center of X-ray emission is flagged as ‘×’. (b) Bubble plot showing the degree of difference between the local velocity distribution for groups of six nearest neighbors and the overall distribution.

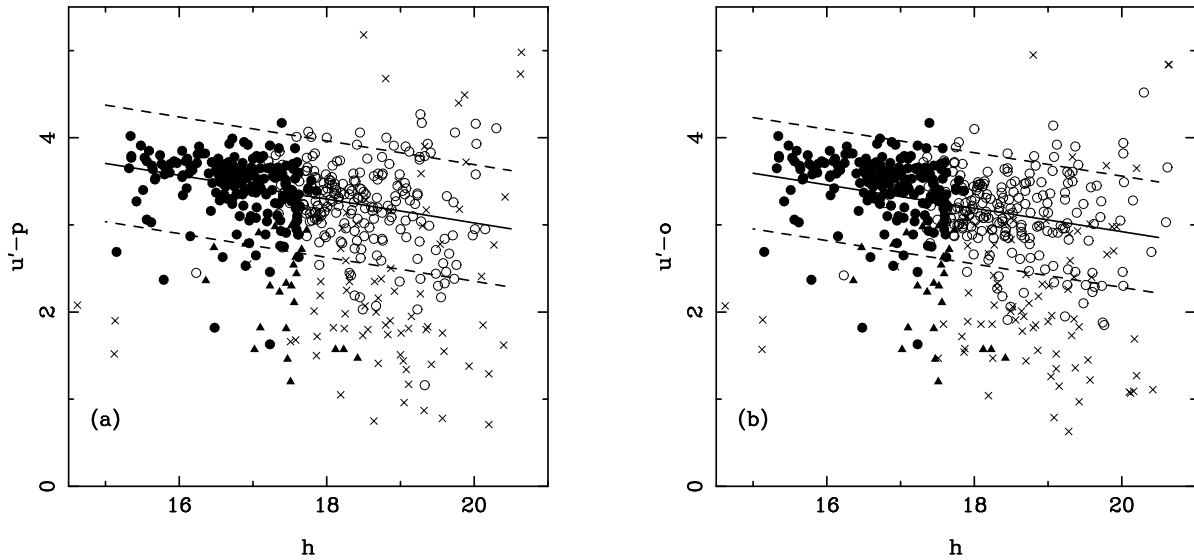


Fig. 12.— Color-magnitude relation for all member galaxies in Abell 2255, i.e., the plots of color indices $u' - p$ and $u' - o$ versus h magnitude for 188 known early-types (filled circles), 26 known late-types (filled triangles), 188 newly-selected early-types (open circles) and 46 newly-selected late-types (crosses).

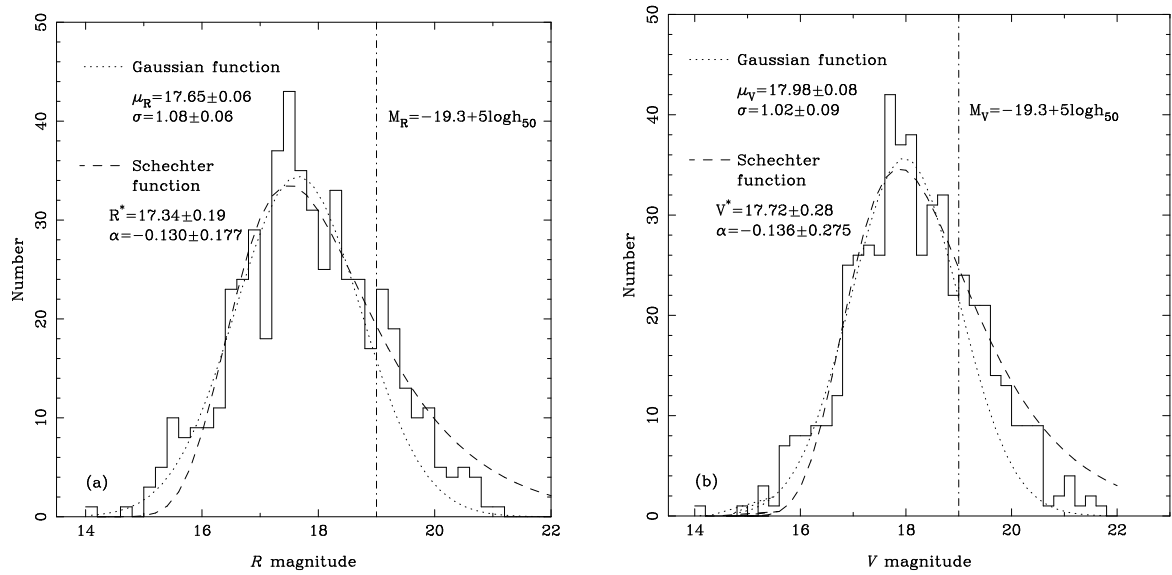


Fig. 13.— Distribution of *R* and *V* magnitudes for all cluster galaxies in Abell 2255.

Table 2. The combined SEDs of 254 known galaxies in the region of Abell 2255

No. (1)	R.A. (2)	Decl. (3)	z_{sp} (4)	z_{phot} (5)	b (6)	d (7)	e (8)	f (9)	g (10)	h (11)	i (12)	j (13)	k (14)	m (15)	n (16)	o (17)	p (18)	u' (19)	g' (20)	r' (21)	i' (22)	z' (23)
1	17 12 34.1	64 05 50	0.076180	0.098	18.16	17.78	17.68	17.57	17.65	17.66	17.55	17.17	17.53	17.49	17.66	17.54	17.30	18.59	17.82	17.68	17.44	17.48
2	17 12 36.1	64 05 08	0.082686	0.079	20.07	18.77	18.15	17.90	17.60	17.50	17.26	17.23	17.14	16.97	16.93	16.80	16.55	20.36	18.44	17.52	17.09	16.74
3	17 12 26.4	64 04 56	0.079492	0.083	19.51	18.45	18.05	17.79	17.53	17.33	17.15	17.08	16.99	16.84	16.79	16.66	16.62	20.25	18.34	17.36	16.94	16.59
4	17 12 28.7	64 06 33	0.074143	0.095	18.36	17.83	17.70	17.67	17.60	17.53	17.43	17.03	17.38	17.31	17.25	17.26	17.06	18.59	17.86	17.55	17.29	17.18
5	17 12 33.2	64 04 18	0.084356	0.086	19.96	18.94	18.39	18.15	17.96	17.81	17.57	17.52	17.40	17.24	17.13	17.06	16.98	20.48	18.82	17.81	17.38	16.98
6	17 12 34.9	64 04 14	0.082410	0.083	18.02	16.88	16.31	16.06	15.78	15.65	15.42	15.35	15.24	15.07	14.98	14.89	14.77	18.69	16.67	15.66	15.21	14.85
7	17 12 41.0	64 04 22	0.083474	0.083	18.74	17.53	16.94	16.70	16.41	16.31	16.07	16.01	15.90	15.75	15.70	15.56	15.46	19.34	17.29	16.30	15.88	15.52
8	17 12 28.8	64 03 39	0.073363	0.068	17.70	16.57	16.03	15.81	15.54	15.41	15.20	15.12	15.02	14.85	14.81	14.69	14.55	18.38	16.38	15.41	15.00	14.66
9	17 12 24.0	64 03 34	0.086135	0.079	20.33	18.96	18.39	18.16	17.88	17.80	17.55	17.44	17.31	17.24	17.19	17.01	17.00	20.47	18.77	17.76	17.33	16.90
10	17 12 51.2	64 04 23	0.073791	0.078	18.27	17.48	17.04	16.84	16.58	16.46	16.25	16.06	16.09	15.92	15.88	15.78	15.61	19.23	17.45	16.49	16.02	15.66
11	17 12 08.0	64 05 51	0.079547	0.075	19.49	18.17	17.65	17.45	17.18	17.06	16.85	16.78	16.65	16.54	16.51	16.40	16.33	19.82	17.95	17.02	16.67	16.28
12	17 12 43.6	64 03 13	0.085514	0.065	19.27	18.02	17.50	17.29	17.03	16.92	16.70	16.69	16.53	16.41	16.28	16.24	16.24	19.67	17.85	16.90	16.52	16.17
13	17 12 22.9	64 08 29	0.075213	0.164	18.20	17.60	17.38	17.29	17.21	17.16	17.00	16.69	16.84	16.90	16.81	16.64	18.54	17.58	17.18	16.86	16.70	
14	17 12 50.0	64 03 11	0.073758	0.066	18.24	17.38	16.85	16.64	16.38	16.24	16.05	15.97	15.88	15.72	15.64	15.56	15.42	19.12	17.19	16.25	15.85	15.50
15	17 12 32.1	64 02 19	0.082710	0.086	18.43	17.82	17.25	16.99	16.90	16.80	16.60	16.52	16.40	16.30	16.20	16.16	16.09	19.60	17.71	16.79	16.40	16.06
16	17 12 13.7	64 08 28	0.073561	0.068	18.26	17.28	16.71	16.51	16.24	16.11	15.91	15.84	15.74	15.58	15.53	15.47	15.36	19.01	17.06	16.10	15.73	15.41
17	17 12 07.0	64 03 20	0.082651	0.076	18.68	17.65	17.17	16.94	16.67	16.54	16.32	16.24	16.16	16.00	15.95	15.83	15.73	19.40	17.49	16.55	16.12	15.76
18	17 11 58.1	64 05 21	0.079605	0.063	18.44	17.27	16.80	16.58	16.29	16.17	15.95	15.87	15.76	15.61	15.51	15.44	15.32	19.15	17.13	16.16	15.75	15.38
19	17 12 19.3	64 02 08	0.082624	0.068	17.69	16.83	16.30	16.07	15.85	15.73	15.51	15.45	15.36	15.22	15.14	15.05	14.98	18.59	16.68	15.73	15.34	15.00
20	17 12 28.3	64 01 52	0.086784	0.082	17.96	17.90	17.12	16.89	16.86	16.80	16.58	16.49	16.42	16.29	16.18	16.06	16.00	19.66	17.79	16.81	16.38	16.02
21	17 12 23.2	64 01 57	0.079710	0.066	18.28	17.16	16.61	16.38	16.10	15.99	15.77	15.68	15.59	15.43	15.35	15.27	15.15	18.94	16.94	15.99	15.57	15.18
22	17 12 16.2	64 02 12	0.071733	0.064	18.07	17.06	16.51	16.33	16.05	15.93	15.72	15.63	15.55	15.36	15.31	15.20	15.10	18.77	16.85	15.94	15.51	15.10
23	17 13 05.5	64 05 28	0.082106	0.066	19.25	18.01	17.49	17.26	16.96	16.84	16.63	16.53	16.45	16.28	16.23	16.11	16.05	19.80	17.86	16.85	16.42	16.06
24	17 13 03.8	64 07 02	0.080867	0.082	18.04	16.97	16.47	16.24	15.95	15.81	15.59	15.51	15.40	15.26	15.17	15.07	14.95	18.83	18.80	15.83	15.36	15.03
25	17 12 57.7	64 03 04	0.073865	0.083	19.27	17.93	17.56	17.28	17.09	16.97	16.74	16.72	16.63	16.46	16.42	16.30	16.21	19.89	17.87	16.97	16.61	16.29
26	17 12 30.4	64 09 31	0.082360	0.063	18.92	17.96	17.70	17.54	17.32	17.21	17.04	16.92	16.94	16.76	16.67	16.49	19.40	18.02	17.21	16.91	16.65	
27	17 12 06.9	64 08 32	0.082294	0.084	18.75	17.97	17.62	17.39	17.23	17.10	16.95	16.90	16.80	16.70	16.64	16.68	16.75	19.48	17.81	17.08	16.81	16.53
28	17 13 07.4	64 05 01	0.0457346	0.461	21.12	22.05	21.39	20.49	20.21	19.66	19.02	18.75	18.82	18.46	18.22	18.41	21.96	21.27	19.60	18.77	18.40	
29	17 12 06.7	64 02 25	0.050839	0.086	18.73	18.25	17.52	17.15	16.96	16.88	16.61	16.57	16.47	16.31	16.24	16.11	16.06	20.02	18.03	16.90	16.43	16.06
30	17 13 02.0	64 03 08	0.082390	0.083	17.92	16.83	16.27	16.03	15.76	15.62	15.39	15.32	15.21	15.06	14.99	14.89	14.76	18.56	16.61	15.61	15.20	14.83
31	17 12 04.8	64 08 43	0.079323	0.067	19.16	18.08	17.64	17.42	17.17	17.05	16.82	16.75	16.67	16.51	16.51	16.36	16.26	19.76	17.96	17.03	16.66	16.33
32	17 11 57.7	64 03 21	0.083442	0.075	18.99	17.96	17.40	17.15	16.88	16.77	16.54	16.45	16.35	16.20	16.10	16.06	15.87	19.64	17.73	16.77	16.33	15.94
33	17 13 01.3	64 02 53	0.082440	0.079	20.29	19.09	18.55	18.28	18.05	17.93	17.71	17.64	17.56	17.39	17.41	17.25	17.16	20.63	18.97	17.95	17.51	17.17
34	17 12 55.5	64 01 57	0.081061	0.082	19.22	18.39	18.14	18.00	17.84	17.72	17.52	17.37	17.23	17.19	17.15	17.08	16.88	19.68	18.34	17.63	17.31	17.15
35	17 12 30.5	64 01 00	0.082146	0.083	19.15	17.96	17.43	17.20	16.93	16.81	16.57	16.50	16.43	16.25	16.17	16.13	15.95	19.80	17.81	16.82	16.40	16.03
36	17 12 01.0	64 02 16	0.074845	0.068	18.82	17.65	17.23	17.06	16.79	16.67	16.48	16.42	16.33	16.19	16.16	16.07	16.00	19.52	17.62	16.69	16.29	15.95
37	17 12 55.4	64 01 45	0.081009	0.079	19.75	18.56	18.12	17.89	17.65	17.46	17.26	17.19	17.08	16.93	16.92	16.75	16.76	20.41	18.42	17.47	17.06	16.71
38	17 11 48.3	64 04 31	0.087262	0.079	18.84	18.57	18.13	17.90	17.63	17.50	17.28	17.20	17.16	17.00	16.84	16.85	16.65	20.24	18.46	17.50	17.12	16.77
39	17 11 55.3	64 08 30	0.082920	0.079	19.89	18.63	18.20	17.96	17.74	17.60	17.39	17.31	17.26	17.13	17.07	16.94	16.81	20.58	18.55	17.58	17.25	16.94
40	17 13 15.2	64 04 24	0.082837	0.079	18.04	17.01	16.50	16.25	16.00	15.86	15.65	15.59	15.47	15.33	15.22	15.15	15.04	18.78	16.82	15.88	15.44	15.12
41	17 11 44.2	64 06 44	0.083267	0.065	16.66	15.86	15.60	15.48	15.29	15.20	15.05	14.95	14.94	14.82	14.76	14.74	14.64	17.40	15.96	15.14	14.98	14.73
42	17 12 18.5	64 09 29	0.080939	0.080	19.37	18.64	18.09	17.90	17.62	17.50	17.30	17.21	17.09	17.00	16.99	16.86	16.79	20.32	18.44	17.50	17.07	16.72
43	17 13 19.0	64 04 37	0.081055	0.078	18.00	16.87	16.34	16.09	15.83	15.71	15.48	15.43	15.31	15.16	15.10	15.01	14.88	18.60	16.68	15.71	14.98	
44	17 11 41.7	64 04 59	0.083371	0.078	18.83	17.77	17.26	17.04	16.76	16.65	16.43	16.34	16.									

Table 2—Continued

No. (1)	R.A. (2)	Decl. (3)	z_{sp} (4)	z_{phot} (5)	b (6)	d (7)	e (8)	f (9)	g (10)	h (11)	i (12)	j (13)	k (14)	m (15)	n (16)	o (17)	p (18)	u' (19)	g' (20)	r' (21)	i' (22)	z' (23)
52	17 11 48.7	64 09 09	0.082817	0.086	18.05	17.20	16.92	16.74	16.56	16.41	16.25	16.15	16.11	15.99	15.96	15.82	15.83	18.27	17.11	16.45	16.05	15.87
53	17 13 12.9	64 01 43	0.076953	0.067	19.30	17.91	17.45	17.23	16.97	16.85	16.64	16.57	16.49	16.30	16.30	16.16	16.04	19.67	17.79	16.87	16.45	16.12
54	17 13 02.6	64 10 52	0.083138	0.083	19.33	18.40	18.03	17.82	17.54	17.44	17.21	17.19	17.10	16.94	16.89	16.77	16.62	19.76	18.32	17.47	17.05	16.80
55	17 11 49.6	64 10 05	0.077127	0.083	17.59	18.52	17.61	17.62	17.40	17.47	17.24	17.30	17.24	17.06	17.01	16.94	16.84	20.20	18.43	17.54	17.14	16.84
56	17 11 38.0	64 02 46	0.078579	0.066	18.98	17.88	17.40	17.17	16.88	16.77	16.53	16.43	16.34	16.17	16.11	15.97	15.86	19.92	17.76	16.78	16.30	15.92
57	17 13 27.9	64 07 21	0.077519	0.079	19.75	18.84	18.27	18.10	17.78	17.62	17.43	17.36	17.31	17.14	17.02	16.94	16.85	20.57	18.62	17.67	17.24	16.97
58	17 12 54.4	63 59 33	0.082869	0.082	18.05	16.99	16.49	16.23	15.98	15.86	15.64	15.56	15.47	15.32	15.25	15.15	15.07	18.72	16.80	15.85	15.45	15.09
59	17 11 34.3	64 08 28	0.080741	0.082	19.81	18.54	18.06	17.80	17.56	17.41	17.21	17.08	17.01	16.88	16.78	16.64	16.53	20.48	18.38	17.44	16.96	16.60
60	17 13 29.1	64 02 49	0.078800	0.082	17.78	16.80	16.22	15.98	15.71	15.60	15.38	15.29	15.19	15.02	14.97	14.85	14.75	18.60	16.56	15.64	15.13	14.81
61	17 12 09.3	63 58 58	0.078832	0.063	19.57	18.55	17.98	17.82	17.56	17.44	17.23	17.12	17.14	16.93	16.84	16.77	16.73	20.36	18.38	17.46	17.08	16.70
62	17 11 39.6	64 10 07	0.076752	0.087	19.66	18.84	18.44	18.33	18.09	17.96	17.75	17.55	17.49	17.38	17.28	17.19	17.08	20.20	18.72	17.95	17.47	17.13
63	17 13 20.5	64 00 34	0.079890	0.104	18.17	17.73	17.62	17.59	17.61	17.59	17.52	17.25	17.51	17.44	17.46	17.15	18.41	17.73	17.62	17.43	17.48	
64	17 13 35.7	64 08 03	0.077916	0.076	18.98	18.12	17.66	17.46	17.20	17.06	16.86	16.82	16.74	16.58	16.41	16.43	16.27	19.73	17.96	17.09	16.69	16.42
65	17 12 01.1	63 58 50	0.082649	0.080	19.95	18.66	18.12	17.91	17.66	17.53	17.30	17.21	17.13	16.99	16.85	16.79	16.80	20.29	18.42	17.52	17.11	16.75
66	17 11 36.2	64 01 00	0.069866	0.064	18.88	18.03	17.51	17.32	17.05	16.91	16.70	16.61	16.53	16.35	16.33	16.24	16.08	19.75	17.84	16.92	16.50	16.14
67	17 12 28.5	63 57 49	0.085724	0.084	19.53	18.59	18.08	17.81	17.60	17.41	17.22	17.09	17.02	16.92	16.82	16.69	16.58	20.31	18.36	17.42	16.99	16.63
68	17 13 10.2	63 59 07	0.081495	0.061	19.20	18.13	17.67	17.47	17.18	17.07	16.85	16.77	16.68	16.55	16.44	16.39	16.28	19.92	17.97	17.06	16.67	16.29
69	17 13 39.1	64 08 00	0.081870	0.079	19.64	18.44	17.90	17.64	17.40	17.26	17.01	16.99	16.85	16.70	16.50	16.52	16.34	20.10	18.25	17.27	16.81	16.46
70	17 13 17.1	64 11 37	0.084017	0.075	18.97	17.96	17.46	17.23	16.94	16.80	16.59	16.53	16.39	16.24	16.16	16.07	15.93	19.70	17.79	16.82	16.35	16.00
71	17 13 43.0	64 04 55	0.084574	0.068	18.35	17.22	16.71	16.47	16.18	16.06	15.82	15.75	15.65	15.48	15.41	15.31	15.18	19.09	17.07	16.08	15.61	15.26
72	17 13 43.5	64 05 02	0.090206	0.080	19.78	18.68	18.30	18.08	17.82	17.68	17.45	17.41	17.29	17.15	17.08	17.01	16.83	19.79	18.48	17.64	17.31	17.20
73	17 11 20.0	64 07 34	0.081090	0.073	19.47	18.50	18.03	17.77	17.57	17.43	17.22	17.12	17.09	16.85	16.85	16.76	16.73	20.42	18.41	17.46	17.03	16.69
74	17 13 43.7	64 07 25	0.080635	0.073	19.76	18.70	18.17	17.91	17.62	17.52	17.31	17.25	17.12	16.93	17.01	16.84	16.70	20.47	18.46	17.52	17.11	16.77
75	17 12 51.0	63 57 38	0.081265	0.070	19.72	18.68	18.22	18.01	17.72	17.62	17.39	17.30	17.24	17.06	17.06	16.91	16.81	20.57	18.54	17.61	17.22	16.89
76	17 11 17.9	64 08 00	0.082396	0.080	17.47	16.55	16.22	16.05	15.81	15.67	15.48	15.37	15.31	15.19	15.18	15.06	14.97	18.08	16.53	15.65	15.31	15.04
77	17 11 45.1	64 12 16	0.082057	0.073	19.32	18.31	18.00	17.90	17.70	17.61	17.47	17.38	17.33	17.24	17.17	17.14	17.06	19.67	18.26	17.67	17.26	17.04
78	17 13 13.4	63 58 37	0.077580	0.079	19.06	18.49	18.08	17.83	17.66	17.58	17.35	17.31	17.22	17.11	17.03	16.99	16.96	20.32	18.48	17.58	17.19	16.88
79	17 13 38.8	64 09 32	0.076793	0.068	19.37	18.27	17.75	17.56	17.32	17.14	16.95	16.86	16.82	16.64	16.60	16.52	16.43	19.93	18.11	17.16	16.78	16.44
80	17 13 33.9	64 00 48	0.082015	0.076	18.34	17.29	16.79	16.54	16.28	16.16	15.95	15.85	15.75	15.59	15.54	15.43	15.36	19.17	17.12	16.16	15.73	15.43
81	17 11 59.8	63 57 54	0.087113	0.068	19.14	18.15	17.77	17.54	17.31	17.16	16.98	16.91	16.83	16.61	16.63	16.56	16.44	19.93	18.08	17.18	16.80	16.41
82	17 13 37.5	64 01 20	0.078600	0.097	19.78	19.13	18.81	18.60	18.63	18.49	18.32	17.94	18.23	18.19	18.18	18.15	18.23	19.79	18.90	18.53	18.12	18.08
83	17 11 24.3	64 10 24	0.079547	0.075	18.53	17.59	17.06	16.82	16.53	16.41	16.18	16.12	16.01	15.83	15.77	15.66	15.53	19.43	17.43	16.44	15.96	15.61
84	17 12 38.1	64 14 30	0.075927	0.065	18.47	17.43	16.94	16.74	16.44	16.32	16.12	16.05	15.92	15.75	15.66	15.59	15.40	19.13	17.22	16.32	15.90	15.59
85	17 11 56.0	63 57 29	0.073778	0.053	18.83	17.70	17.33	17.20	16.97	16.88	16.71	16.66	16.60	16.39	16.33	16.22	16.19	19.39	17.61	16.89	16.57	16.27
86	17 13 52.0	64 07 10	0.082871	0.083	18.89	18.15	17.99	17.87	17.72	17.65	17.52	17.43	17.31	17.27	17.24	17.25	16.99	19.17	18.12	17.65	17.31	17.17
87	17 13 48.2	64 08 50	0.095193	0.086	20.01	18.37	17.91	17.59	17.28	17.19	16.98	16.93	16.84	16.70	16.58	16.48	16.30	20.17	18.24	17.23	16.80	16.46
88	17 13 25.3	63 58 43	0.079154	0.070	19.26	18.24	17.80	17.60	17.35	17.25	17.04	16.99	16.94	16.74	16.70	16.71	16.57	19.96	18.14	17.26	16.90	16.57
89	17 11 07.4	64 04 57	0.082762	0.079	19.02	18.30	17.60	17.38	17.12	17.10	16.83	16.75	16.68	16.52	16.45	16.35	16.32	20.18	18.08	17.06	16.68	16.28
90	17 13 48.0	64 01 33	0.071777	0.068	19.64	18.66	18.22	18.07	17.77	17.69	17.48	17.42	17.27	17.17	17.07	17.02	16.82	20.25	18.51	17.67	17.27	17.01
91	17 13 42.7	64 00 21	0.057218	0.416	23.13	20.48	20.04	19.95	19.51	19.45	19.04	19.05	18.92	18.77	18.97	18.59	18.44	21.46	22.39	19.55	18.78	18.42
92	17 13 31.5	64 12 21	0.084550	0.079	19.00	17.51	17.03	16.74	16.47	16.34	16.10	16.05	15.92	15.75	15.67	15.58	15.42	19.41	17.35	16.35	15.88	15.52
93	17 13 57.3	64 06 41	0.080820	0.086	18.44	18.18	17.72	17.47	17.21	17.05	16.84	16.72	16.68	16.52	16.39	16.35	16.23	19.88	18.04	17.07	16.63	16.27
94	17 13 48.2	64 01 13	0.081958	0.076	18.84	17.87	17.36	17.12	16.84	16.74	16.50	16.43	16.32	16.18	16.12	16.02	15.90	19.69	17.68	16.74	16.30	15.98
95	17 12 48.8	63 56 17	0.070615	0.065	19.19	18.11	17.69	17.53	17.30	17.18	17.00	16.92										

Table 2—Continued

No. (1)	R.A. (2)	Decl. (3)	z_{sp} (4)	z_{phot} (5)	b (6)	d (7)	e (8)	f (9)	g (10)	h (11)	i (12)	j (13)	k (14)	m (15)	n (16)	o (17)	p (18)	u' (19)	g' (20)	r' (21)	i' (22)	z' (23)
103	17 12 24.5	64 16 00	0.055060	0.049	16.93	16.02	15.64	15.49	15.21	15.07	14.85	14.77	14.55	14.47	14.35	14.27	17.70	16.00	15.10	14.70	14.39	
104	17 13 13.2	63 56 10	0.119362	0.053	19.13	18.25	17.93	17.78	17.56	17.47	17.31	17.24	17.18	17.04	17.04	16.87	16.88	20.31	18.63	17.57	17.07	16.61
105	17 13 54.3	64 00 17	0.087072	0.076	19.15	18.00	17.59	17.40	17.18	17.04	16.85	16.82	16.75	16.61	16.58	16.44	16.50	19.68	17.87	17.08	16.69	16.43
106	17 11 01.7	64 01 34	0.095427	0.086	18.46	17.32	16.89	16.59	16.36	16.20	15.98	15.89	15.80	15.67	15.59	15.43	15.32	19.06	17.19	16.19	15.78	15.42
107	17 11 01.3	64 01 05	0.095596	0.088	19.63	18.57	18.07	17.80	17.59	17.41	17.23	17.13	17.06	16.96	16.91	16.70	16.59	19.92	18.29	17.40	17.06	16.71
108	17 13 12.8	63 55 40	0.119264	0.090	19.74	18.46	17.91	17.58	17.41	17.22	16.96	16.91	16.80	16.71	16.55	16.48	16.39	20.12	18.15	17.18	16.81	16.50
109	17 10 53.5	64 03 05	0.081013	0.067	18.81	17.84	17.35	17.10	16.80	16.67	16.46	16.36	16.28	16.10	16.02	15.94	15.78	19.53	17.65	16.68	16.25	15.89
110	17 13 05.1	63 55 16	0.080004	0.067	20.35	18.74	18.24	18.05	17.76	17.63	17.42	17.30	17.29	17.06	17.01	16.91	16.87	20.48	18.59	17.64	17.25	16.91
111	17 11 27.9	64 14 12	0.073057	0.068	19.26	18.38	17.92	17.78	17.49	17.40	17.18	17.10	17.02	16.85	16.86	16.76	16.53	20.18	18.33	17.41	16.99	16.70
112	17 13 26.1	64 15 07	0.078691	0.078	19.53	18.78	18.26	18.10	17.83	17.66	17.47	17.44	17.36	17.19	17.27	16.98	17.14	20.26	18.64	17.69	17.31	17.02
113	17 11 07.3	63 59 02	0.082554	0.079	18.97	17.92	17.47	17.22	16.95	16.81	16.60	16.52	16.41	16.26	16.09	16.03	19.57	17.77	16.82	16.38	16.02	
114	17 14 16.1	64 05 38	0.085454	0.088	19.01	18.06	17.83	17.69	17.50	17.43	17.22	17.20	17.10	17.04	16.96	16.87	16.99	19.30	18.10	17.44	17.07	16.88
115	17 11 59.3	64 16 36	0.081569	0.085	18.14	17.87	17.56	17.47	17.41	17.31	17.18	17.00	17.15	17.00	16.94	16.92	16.71	20.69	17.94	17.39	17.02	16.93
116	17 12 08.3	64 16 53	0.076413	0.068	17.56	16.54	16.04	15.82	15.53	15.39	15.19	15.12	15.01	14.84	14.77	14.70	14.57	18.30	16.35	15.40	14.98	14.63
117	17 14 19.4	64 04 15	0.079025	0.076	19.15	18.38	17.84	17.58	17.34	17.22	17.01	16.94	16.80	16.68	16.62	16.55	16.41	20.02	18.16	17.21	16.79	16.45
118	17 11 49.0	63 54 35	0.078904	0.065	19.15	18.16	17.66	17.42	17.17	17.05	16.82	16.73	16.62	16.47	16.39	16.30	16.16	19.99	17.99	17.04	16.62	16.21
119	17 14 03.8	63 59 13	0.077172	0.074	13.57	17.98	17.42	17.19	16.89	16.75	16.52	16.45	16.29	16.14	16.07	15.97	15.81	19.83	17.73	16.75	16.27	15.89
120	17 13 51.9	64 13 47	0.075808	0.070	18.73	17.82	17.33	17.15	16.85	16.70	16.48	16.38	16.29	16.12	16.03	15.99	15.85	19.49	17.70	16.73	16.24	15.90
121	17 13 45.5	64 14 47	0.095226	0.136	18.17	17.51	17.44	17.34	17.32	17.30	17.17	17.22	17.14	17.09	17.08	16.96	16.82	18.53	17.68	17.37	17.06	17.06
122	17 13 19.9	63 54 28	0.090434	0.078	16.89	15.97	15.72	15.58	15.41	15.33	15.14	15.06	15.01	14.86	14.91	14.72	14.62	17.39	16.13	15.26	15.06	14.80
123	17 12 19.7	64 17 56	0.077170	0.066	18.54	17.82	17.14	16.97	16.74	16.62	16.42	16.38	16.33	16.09	16.06	15.99	15.92	19.32	17.58	16.67	16.25	15.93
124	17 13 31.3	64 16 20	0.081115	0.063	19.18	18.25	17.77	17.56	17.28	17.16	16.95	16.92	16.79	16.63	16.56	16.50	16.40	20.00	18.09	17.18	16.76	16.42
125	17 14 16.6	64 00 37	0.078761	0.078	19.34	18.31	17.82	17.59	17.31	17.18	16.97	16.90	16.76	16.66	16.49	16.52	16.34	19.84	18.07	17.20	16.73	16.41
126	17 12 36.3	64 18 33	0.075653	0.087	19.19	18.30	18.06	17.95	17.82	17.68	17.54	17.45	17.47	17.33	17.22	16.98	16.98	18.28	17.73	17.40	17.21	17.21
127	17 14 09.5	64 13 12	0.078953	0.068	18.89	17.81	17.27	17.04	16.76	16.63	16.42	16.33	16.25	16.06	16.01	15.92	15.85	19.43	17.58	16.66	16.20	15.85
128	17 14 04.5	64 14 11	0.087764	0.089	16.78	18.42	18.01	17.80	17.63	17.39	17.16	17.12	17.00	16.90	16.87	16.71	16.77	19.97	18.26	17.39	16.98	16.67
129	17 11 47.1	63 53 05	0.090679	0.082	18.87	17.93	17.49	17.23	17.00	16.86	16.63	16.54	16.45	16.31	16.27	16.10	16.04	19.74	17.76	16.83	16.45	16.06
130	17 11 34.5	63 53 38	0.076627	0.078	18.80	17.94	17.70	17.56	17.37	17.28	17.09	16.84	16.79	16.60	16.55	16.47	16.34	19.13	17.95	17.31	16.87	16.60
131	17 14 30.7	64 10 09	0.079308	0.076	19.57	18.31	17.78	17.57	17.27	17.17	16.94	16.91	16.79	16.64	16.46	16.44	16.32	20.06	18.14	17.19	16.75	16.44
132	17 12 35.7	63 51 39	0.080814	0.079	19.52	18.45	18.21	18.06	17.90	17.79	17.62	17.49	17.43	17.34	17.38	17.20	17.02	20.01	18.49	17.83	17.38	17.11
133	17 12 25.7	64 19 46	0.076930	0.075	18.15	17.29	16.74	16.51	16.24	16.10	15.89	15.82	15.75	15.56	15.51	15.45	15.34	18.96	17.05	16.13	15.69	15.39
134	17 12 12.9	64 19 51	0.077759	0.067	19.00	17.90	17.30	17.09	16.79	16.65	16.44	16.35	16.27	16.09	16.05	15.94	15.80	19.55	17.63	16.67	16.23	15.91
135	17 14 05.6	64 16 02	0.0246861	0.211	19.03	19.57	19.02	18.85	18.80	17.55	17.07	16.81	16.53	16.37	16.13	16.02	15.93	15.77	15.55	15.42	19.31	17.45
136	17 10 33.2	63 58 27	0.082779	0.067	18.91	17.92	17.51	17.30	17.05	16.92	16.72	16.64	16.56	16.42	16.41	16.25	16.22	19.51	17.82	16.92	16.54	16.23
137	17 11 35.6	63 51 54	0.088507	0.093	17.95	17.01	16.69	16.52	16.32	16.21	16.02	15.93	15.87	15.75	15.65	15.55	15.45	18.49	17.12	16.21	15.84	15.55
138	17 13 01.8	63 50 54	0.078901	0.150	19.33	18.51	18.34	18.23	18.20	18.18	18.02	17.67	17.97	17.91	18.11	17.85	17.69	19.34	18.52	18.21	17.87	17.73
139	17 14 46.2	64 08 41	0.072758	0.083	18.24	17.27	16.77	16.45	16.21	16.17	15.96	15.91	15.85	15.71	15.58	15.53	15.39	18.89	17.08	16.18	15.81	15.49
140	17 11 23.0	63 52 28	0.089996	0.082	18.71	17.59	17.11	16.84	16.61	16.48	16.26	16.15	16.07	15.93	15.86	15.72	15.57	19.28	17.48	16.46	16.06	15.69
141	17 10 33.1	63 57 42	0.083903	0.079	18.29	17.17	16.69	16.44	16.15	16.02	15.79	15.69	15.59	15.43	15.36	15.24	15.11	18.89	17.02	16.02	15.56	15.20
142	17 11 29.6	63 51 58	0.089188	0.083	18.80	17.55	17.07	16.81	16.53	16.37	16.13	16.02	15.93	15.77	15.69	15.55	15.42	19.31	17.45	16.37	15.90	15.51
143	17 11 23.1	64 19 06	0.076404	0.063	18.98	17.95	17.49	17.29	17.00	16.89	16.68	16.61	16.51	16.37	16.30	16.20	16.09	19.67	17.80	16.91	16.47	16.17
144	17 11 48.1	64 20 21	0.077186	0.070	19.32	18.66	18.15	17.99	17.71	17.58	17.37	17.32	17.20	17.03	17.00	16.91	16.74	20.24	18.44	17.57	17.19	16.89
145	17 12 45.1	64 21 07	0.076309	0.068	19.19	18.10	17.68	17.53	17.27	17.11	16.96	16.92	16.84	16.69	16.71	16.56	16.48	19.63	17.97	17.13	16.80	16.56
146	17 10 08.1	64 03 11	0.077900	0.061	18.55	17.62	17.10	16.90	16.62</td													

Table 2—Continued

No. (1)	R.A. (2)	Decl. (3)	z_{sp} (4)	z_{phot} (5)	b (6)	d (7)	e (8)	f (9)	g (10)	h (11)	i (12)	j (13)	k (14)	m (15)	n (16)	o (17)	p (18)	u' (19)	g' (20)	r' (21)	i' (22)	z' (23)	
154	17 13 09.9	63 49 40	0.082734	0.077	19.07	18.45	17.99	17.76	17.47	17.36	17.15	17.03	16.86	16.78	16.82	16.60	16.58	20.20	18.25	17.31	16.90	16.54	
155	17 12 23.0	63 49 06	0.150721	0.092	19.25	18.45	18.18	17.98	17.85	17.76	17.54	17.47	17.15	17.32	17.28	17.10	17.17	19.61	18.33	17.66	17.25	16.98	
156	17 10 10.3	64 11 47	0.171484	0.191	21.39	20.50	19.58	19.54	19.36	19.72	19.43	19.40	19.35	19.39	18.94	19.15	19.37	20.70	20.30	19.76	19.27	19.06	
157	17 12 44.9	64 22 10	0.076335	0.068	19.48	18.36	17.94	17.76	17.45	17.32	17.15	17.04	17.00	16.85	16.77	16.75	16.64	20.11	18.23	17.35	16.95	16.67	
158	17 11 45.9	64 21 32	0.082031	0.083	18.11	17.02	16.50	16.25	15.96	15.82	15.61	15.52	15.43	15.26	15.19	15.10	14.99	18.78	16.82	15.84	15.40	15.07	
159	17 15 01.0	64 09 03	0.209854	0.206	19.41	19.48	18.59	18.19	17.83	17.77	17.44	17.39	17.35	17.13	17.00	16.81	17.08	21.43	19.16	17.81	17.26	16.94	
160	17 14 57.2	64 00 34	0.084235	0.068	19.12	18.16	17.70	17.50	17.21	17.11	16.86	16.78	16.70	16.56	16.53	16.43	16.37	19.82	18.01	17.13	16.66	16.33	
161	17 15 00.1	64 10 08	0.079925	0.078	19.84	18.80	18.21	18.09	17.82	17.71	17.48	17.42	17.33	17.19	17.08	17.12	17.04	20.34	18.56	17.69	17.32	17.09	
162	17 10 57.4	63 51 59	0.082913	0.098	18.17	17.41	17.25	17.20	17.15	17.08	16.99	16.81	16.96	16.85	16.84	16.77	16.72	18.36	17.50	17.15	16.85	16.75	
163	17 12 42.9	63 48 35	0.074926	0.097	17.75	16.96	16.76	16.66	16.62	16.55	16.42	16.10	16.31	16.28	16.30	16.22	16.13	18.02	16.94	16.57	16.24	16.10	
164	17 15 05.0	64 02 42	0.080506	0.078	19.76	18.36	17.84	17.59	17.29	17.17	16.93	16.86	16.75	16.58	16.62	16.50	16.34	20.22	18.11	17.19	16.70	16.36	
165	17 14 29.1	64 16 56	0.089946	0.082	18.60	17.71	17.37	17.16	16.99	16.85	16.65	16.59	16.52	16.40	16.33	16.27	16.14	19.12	17.67	16.89	16.45	16.24	
166	17 13 37.2	63 49 51	0.085908	0.076	19.52	18.17	17.77	17.54	17.36	17.26	17.09	17.04	16.95	16.82	16.82	16.75	16.67	19.78	18.06	17.27	16.92	16.59	
167	17 10 58.0	63 51 33	0.080911	0.068	18.39	17.70	17.18	17.00	16.78	16.67	16.47	16.40	16.32	16.15	16.17	16.01	15.89	19.30	17.55	16.69	16.27	15.94	
168	17 15 09.1	64 02 53	0.079963	0.079	17.81	16.77	16.19	15.96	15.66	15.55	15.31	15.26	15.13	14.96	14.92	14.81	14.67	18.66	16.52	15.57	15.08	14.76	
169	17 13 33.9	63 49 26	0.086203	0.070	17.39	16.40	16.07	15.92	15.72	15.62	15.45	15.38	15.28	15.17	15.17	15.03	14.89	18.03	16.41	15.62	15.27	14.93	
170	17 14 49.4	63 56 20	0.220828	0.211	20.40	19.36	18.72	18.31	17.79	17.71	17.37	17.28	17.17	17.00	16.94	16.67	16.70	21.63	19.20	17.71	17.13	16.80	
171	17 12 26.4	64 23 23	0.078059	0.065	19.15	18.01	17.45	17.23	16.98	16.84	16.65	16.60	16.50	16.32	16.25	16.18	16.05	19.50	17.79	16.88	16.45	16.15	
172	17 13 20.4	63 48 35	0.084767	0.077	19.07	18.00	17.53	17.27	17.03	16.93	16.69	16.59	16.50	16.35	16.35	16.21	16.10	19.88	17.86	16.90	16.50	16.12	
173	17 13 02.1	63 47 59	0.074543	0.083	19.65	18.56	18.15	17.95	17.69	17.58	17.39	17.26	17.15	17.08	17.12	16.88	16.80	19.88	18.39	17.57	17.15	16.83	
174	17 14 06.3	64 20 18	0.084343	0.094	18.42	17.94	17.83	17.71	17.64	17.51	17.45	17.37	17.30	17.31	17.29	17.26	17.11	19.01	18.02	17.57	17.24	17.09	
175	17 11 29.6	63 48 53	0.119498	0.139	20.13	19.13	18.39	18.07	17.83	17.69	17.45	17.35	17.26	17.16	16.94	16.74	16.78	21.13	18.91	17.72	17.21	16.80	
176	17 10 51.1	63 51 13	0.082934	0.060	19.12	17.99	17.61	17.37	17.07	16.93	16.67	16.51	16.42	16.23	16.17	15.95	15.81	19.82	17.93	16.96	16.37	15.94	
177	17 15 15.9	64 02 22	0.078681	0.072	19.04	17.90	17.41	17.18	16.86	16.78	16.53	16.48	16.36	16.23	16.17	16.09	16.96	17.69	16.75	16.37	16.07		
178	17 13 16.0	63 47 38	0.082905	0.082	17.66	16.56	16.03	15.79	15.52	15.41	15.19	15.08	14.99	14.82	14.79	14.65	14.56	18.42	16.36	15.40	14.98	14.56	
179	17 15 23.9	64 04 16	0.073291	0.066	18.37	17.43	17.02	16.86	16.60	16.49	16.29	16.23	16.12	16.00	15.99	15.93	15.83	19.06	17.32	16.48	16.12	15.82	
180	17 10 36.2	64 20 03	0.077836	0.052	19.19	18.36	18.01	17.84	17.58	17.45	17.27	17.10	17.09	16.95	16.82	16.72	16.63	19.74	18.28	17.49	17.02	16.71	
181	17 13 15.4	64 24 18	0.083182	0.084	18.80	18.04	17.60	17.39	17.15	16.96	16.79	16.68	16.61	16.49	16.40	16.38	16.24	19.09	17.80	17.00	16.56	16.28	
182	17 15 31.5	64 10 34	0.081998	0.079	19.86	18.62	18.21	18.05	17.75	17.67	17.45	17.40	17.28	17.17	17.16	16.99	16.88	20.06	18.51	17.66	17.27	17.06	
183	17 13 42.1	63 46 46	0.081683	0.078	18.89	17.75	17.21	16.95	16.68	16.59	16.34	16.21	16.11	15.94	15.91	15.74	15.60	19.43	17.54	16.56	16.11	15.68	
184	17 15 27.3	64 12 53	0.076226	0.076	19.10	18.31	17.82	17.62	17.35	17.24	17.06	17.02	16.86	16.74	16.70	16.66	16.76	19.73	18.07	17.23	16.86	16.61	
185	17 15 13.4	63 55 03	0.150054	0.144	19.91	18.98	18.36	17.94	17.66	17.51	17.22	17.15	17.01	16.92	16.75	16.71	16.58	20.61	18.67	17.49	17.01	16.66	
186	17 15 39.8	64 03 36	0.080577	0.079	19.16	18.29	17.96	17.77	17.47	17.37	17.18	17.08	17.01	16.87	16.79	16.71	16.57	19.90	18.24	17.36	17.00	16.63	
187	17 14 06.5	63 47 27	0.075649	0.063	17.81	18.28	17.88	17.75	17.52	17.44	17.25	17.20	17.10	16.99	16.95	16.87	16.89	19.91	18.19	17.38	17.15	16.88	
188	17 12 02.8	63 44 38	0.075955	0.063	18.57	17.69	17.30	17.13	16.89	16.78	16.62	16.45	16.44	16.27	16.29	16.13	16.06	19.38	17.71	16.81	16.40	16.05	
189	17 14 55.2	63 51 29	0.074744	0.075	19.95	18.74	18.32	18.12	17.81	17.65	17.38	17.31	17.15	16.99	16.81	16.52	20.48	18.63	17.65	17.12	16.68		
190	17 13 02.3	63 44 09	0.079792	0.063	19.70	18.53	18.14	17.90	17.59	17.52	17.30	17.14	17.09	16.92	16.80	16.75	16.73	20.28	18.44	17.49	17.09	16.70	
191	17 12 03.5	63 44 03	0.075648	0.083	19.61	18.40	18.11	17.95	17.72	17.66	17.45	17.26	17.31	17.18	16.92	16.76	16.67	16.58	19.58	18.40	17.68	17.24	16.93
192	17 15 12.4	64 19 09	0.095025	0.086	19.14	18.11	17.69	17.45	17.19	17.04	16.79	16.75	16.61	16.57	16.39	16.29	16.22	19.72	18.03	17.05	16.59	16.29	
193	17 13 50.8	63 44 51	0.078050	0.065	19.60	18.50	17.96	17.77	17.47	17.37	17.18	17.08	17.01	16.87	16.79	16.71	16.57	19.90	18.24	17.36	17.00	16.63	
194	17 10 40.6	63 46 35	0.081944	0.079	19.59	18.72	18.28	18.02	17.73	17.64	17.44	17.33	17.27	17.12	17.02	16.87	16.86	20.12	18.60	17.65	17.24	16.94	
195	17 15 09.6	64 20 10	0.087847	0.083	18.74	17.79	17.26	16.99	16.70	16.57	16.32	16.24	16.14	16.01	15.89	15.77	15.62	19.39	17.59	16.58	16.10	15.76	
196	17 12 48.4	63 42 58	0.075274	0.068	18.70	17.61	17.26	17.06	16.80	16.68	16.48	16.31	16.27	16.12	16.07	15.96	15.88	19.61	17.70	16.71	16.22	15.83	
197	17 15 28.9	63 53 34	0.079747	0.083	18.91	18.28	17.67																

Table 2—Continued

No. (1)	R.A. (2)	Decl. (3)	z_{sp} (4)	z_{phot} (5)	b (6)	d (7)	e (8)	f (9)	g (10)	h (11)	i (12)	j (13)	k (14)	m (15)	n (16)	o (17)	p (18)	u' (19)	g' (20)	r' (21)	i' (22)	z' (23)	
205	17 14 01.5	63 43 40	0.034081	0.097	17.93	17.37	17.18	17.10	16.99	16.96	16.74	16.69	16.74	16.67	16.72	16.54	16.41	18.52	17.38	16.97	16.69	16.48	
206	17 11 55.2	64 29 27	0.082349	0.063	99.00	17.70	17.40	17.26	17.09	16.97	16.83	16.74	16.72	16.57	16.56	16.46	16.37	18.97	17.69	16.93	16.74	16.54	
207	17 09 00.9	64 13 39	0.315038	0.385	23.00	20.49	20.05	19.58	18.80	18.55	18.25	18.07	18.02	17.66	17.57	17.47	17.28	21.80	20.24	18.58	17.95	17.56	
208	17 16 02.1	63 57 29	0.079818	0.079	19.15	18.25	18.02	17.96	17.71	17.60	17.45	17.34	17.37	17.20	17.23	17.11	17.01	19.40	18.23	17.64	17.31	17.11	
209	17 10 35.9	63 44 25	0.079755	0.063	19.92	18.47	18.14	17.95	17.73	17.65	17.48	17.38	17.33	17.15	17.09	16.96	16.99	20.01	18.48	17.68	17.28	17.01	
210	17 16 18.4	64 07 58	0.075404	0.068	18.10	17.08	16.53	16.34	16.03	15.90	15.69	15.63	15.49	15.35	15.27	15.21	15.05	18.73	16.85	15.90	15.48	15.12	
211	17 16 08.5	63 58 06	0.080688	0.069	18.91	17.89	17.32	17.09	16.77	16.64	16.41	16.35	16.21	16.03	16.00	15.86	15.73	19.42	17.64	16.64	16.19	15.79	
212	17 16 09.4	63 56 41	0.082395	0.070	19.13	18.17	17.62	17.39	17.10	17.00	16.79	16.69	16.57	16.42	16.38	16.32	16.11	19.74	17.91	16.99	16.57	16.27	
213	17 08 37.8	64 01 45	0.454927	0.456	21.99	21.38	20.29	20.48	19.79	19.25	18.75	18.61	18.61	18.47	18.36	18.09	18.30	23.31	20.99	19.31	18.47	18.09	
214	17 15 51.4	63 51 59	0.081804	0.082	19.75	18.53	18.18	17.95	17.75	17.67	17.47	17.38	17.29	17.19	17.13	17.11	16.95	20.32	18.55	17.64	17.29	17.00	
215	17 14 09.6	63 41 57	0.076214	0.070	19.76	18.58	18.10	17.92	17.65	17.59	17.36	17.30	17.24	17.05	17.10	16.95	16.76	20.15	18.43	17.60	17.20	16.88	
216	17 13 49.9	63 41 00	0.359867	0.384	22.02	21.83	20.62	19.65	19.38	18.97	18.73	18.68	18.49	18.48	18.07	18.45	22.21	21.26	19.31	18.68	18.14		
217	17 16 14.8	63 56 41	0.080730	0.078	17.85	16.90	16.35	16.13	15.82	15.70	15.50	15.41	15.31	15.15	15.10	15.01	14.85	18.62	16.68	15.71	15.29	14.91	
218	17 16 18.7	64 14 13	0.076884	0.070	18.97	18.05	17.50	17.32	17.03	16.92	16.70	16.65	16.53	16.40	16.33	16.31	16.09	19.64	17.82	16.91	16.52	16.25	
219	17 10 09.5	63 44 09	0.285630	0.269	20.20	20.27	19.65	18.81	18.20	17.95	17.77	17.55	17.50	17.42	17.34	17.08	16.92	21.90	19.58	18.01	17.42	17.08	
220	17 16 19.0	63 55 35	0.079917	0.083	18.92	18.35	18.06	17.92	17.72	17.65	17.42	17.27	17.23	17.15	17.13	17.16	16.85	19.58	18.33	17.63	17.23	16.93	
221	17 15 46.3	64 22 16	0.034651	0.041	17.92	17.43	17.15	17.09	16.86	16.77	16.55	16.57	16.55	16.44	16.34	16.29	16.21	18.57	17.31	16.84	16.44	16.27	
222	17 11 36.0	63 39 06	0.080320	0.062	17.65	16.48	16.03	15.84	15.57	15.49	15.00	15.18	15.15	14.97	14.97	14.83	14.72	18.07	16.42	15.49	15.13	14.84	
223	17 09 53.8	63 44 28	0.071268	0.062	18.53	17.64	17.29	17.13	16.89	16.78	16.61	16.42	16.42	16.24	16.16	16.16	15.93	19.30	17.63	16.81	16.36	16.04	
224	17 15 38.0	64 23 51	0.080204	0.067	18.81	17.81	17.33	17.13	16.87	16.74	16.47	16.48	16.37	16.22	16.11	16.10	15.96	19.54	17.67	16.76	16.33	16.04	
225	17 16 37.3	64 10 50	0.251235	0.229	22.58	21.30	21.21	20.84	20.32	19.99	19.81	19.86	19.89	19.51	19.38	19.33	22.84	21.74	20.05	19.79	19.45		
226	17 08 18.5	64 07 02	0.360749	0.378	21.53	20.71	20.02	20.10	19.02	18.67	18.38	18.36	18.37	17.98	17.92	17.81	18.03	23.04	20.60	18.79	18.20	17.87	
227	17 11 54.8	64 32 58	0.457453	0.453	99.00	21.66	21.16	20.42	19.98	19.49	19.05	18.88	18.99	18.70	18.92	18.46	18.22	24.60	21.38	19.59	18.81	18.27	
228	17 11 09.2	63 39 16	0.082092	0.075	19.41	18.38	17.95	17.73	17.45	17.41	17.00	16.99	16.84	16.91	16.69	16.66	19.98	18.29	17.41	16.98	16.69		
229	17 16 42.3	64 10 41	0.250627	0.244	21.00	20.41	19.65	19.10	18.48	18.32	18.08	18.04	17.73	17.72	17.67	17.49	21.63	19.77	18.29	17.76	17.46		
230	17 15 01.0	64 28 51	0.103433	0.083	18.83	17.93	17.66	17.43	17.18	16.98	16.77	16.74	16.54	16.48	16.34	16.25	16.17	19.41	17.96	17.02	16.49	16.16	
231	17 10 52.5	63 39 17	0.080758	0.073	18.54	17.57	17.18	16.94	16.72	16.61	16.00	16.27	16.26	16.09	16.10	15.95	15.83	19.18	17.53	16.66	16.20	15.91	
232	17 15 29.5	63 44 53	0.177041	0.076	19.25	18.50	18.10	17.93	17.66	17.64	17.36	17.29	17.20	16.99	17.05	16.90	16.79	19.87	18.50	17.65	17.16	16.86	
233	17 11 13.2	63 38 15	0.078725	0.065	19.14	17.92	17.37	17.16	16.90	16.90	16.46	16.43	16.24	16.20	16.08	16.00	16.69	17.81	16.85	16.38	16.06		
234	17 12 21.1	64 34 18	0.082911	0.073	19.29	18.34	17.92	17.73	17.53	17.36	17.18	17.09	17.11	16.88	16.90	16.83	16.63	19.68	18.16	17.41	17.03	16.71	
235	17 14 24.3	63 39 38	0.081370	0.067	19.18	18.11	17.84	17.72	17.47	17.41	17.00	16.99	16.85	16.91	16.76	16.55	19.73	18.15	17.43	16.92	16.67		
236	17 09 54.0	63 42 29	0.080894	0.065	19.18	18.01	17.67	17.48	17.25	17.14	16.93	16.79	16.82	16.61	16.60	16.49	16.42	19.92	18.04	17.18	16.74	16.45	
237	17 10 37.4	64 31 43	0.078122	0.083	18.81	18.06	17.85	17.76	17.59	17.51	17.37	17.24	17.25	17.09	17.03	17.04	16.84	19.25	18.12	17.54	17.19	16.95	
238	17 09 57.6	63 42 07	0.360057	0.389	21.33	20.48	20.38	20.19	19.47	19.04	18.63	18.55	18.44	18.22	17.98	17.85	22.38	20.98	19.03	18.39	17.98		
239	17 15 41.0	64 26 11	0.080183	0.083	18.77	18.07	17.68	17.51	17.26	17.14	16.91	16.81	16.71	16.59	16.46	16.47	16.33	19.36	18.00	17.14	16.69	16.43	
240	17 14 32.7	63 39 29	0.359913	0.332	0.00	20.53	20.36	20.15	19.17	18.93	0.00	18.57	18.33	18.12	18.14	17.89	18.07	22.16	20.73	18.94	18.32	17.88	
241	17 16 22.1	64 22 13	0.078226	0.065	19.14	18.25	17.75	17.56	17.28	17.13	16.93	16.86	16.78	16.61	16.57	16.47	16.32	19.89	18.04	17.18	16.70	16.39	
242	17 08 45.1	63 47 46	0.054283	0.048	17.72	16.92	16.63	16.56	16.30	16.18	15.97	15.85	15.93	15.72	15.64	15.52	15.48	18.36	16.96	16.21	15.86	15.54	
243	17 08 40.7	64 23 22	0.476510	0.483	23.11	21.99	21.24	21.12	20.06	19.48	19.20	18.87	18.83	18.63	18.41	18.41	18.11	21.54	21.33	19.55	18.72	18.20	
244	17 14 05.8	64 34 55	0.080722	0.058	99.00	18.63	18.15	99.00	99.00	99.00	17.58	17.42	17.30	17.24	17.09	16.97	16.93	16.69	20.09	18.55	17.65	17.15	16.83
245	17 16 05.8	63 44 41	0.234675	0.229	19.67	19.01	18.70	18.33	17.84	17.73	17.49	17.39	17.24	17.08	17.08	16.95	16.94	20.55	19.05	17.77	17.17	16.81	
246	17 15 10.4	64 33 02	0.079069	0.070	19.09	17.84	17.28	17.07	16.71	16.63	16.41	16.36	16.26	16.08	16.01	16.03	15.80	19.43	17.61	16.64	16.23	15.95	
247	17 16 34.8	63 46 36	0.313587	0.300	20.94	20.23	20.43	19.75	19.18	18.80	18.66	18.34	18.19	18.10	18.13	17.75	17.93	21.58	20.56	18.79	18.20	17.77	

Table 4. The combined SEDs of 313 newly-selected member galaxies in the region of Abell 2255

No. (1)	R.A.(J2000) (2)	Decl. (3)	z_{phot} (4)	T (5)	b (6)	d (7)	e (8)	f (9)	g (10)	h (11)	i (12)	j (13)	k (14)	m (15)	n (16)	σ (17)	p (18)	u' (19)	g' (20)	r' (21)	i' (22)	z' (23)		
1	17 16 02.36	63 57 55.04	0.079	2	19.85	19.00	18.77	18.62	18.29	18.21	17.98	17.87	17.80	17.58	17.72	17.55	17.41	20.20	18.90	18.16	17.82	17.76		
2	17 10 16.85	64 21 07.74	0.073	3	20.40	20.01	19.44	19.23	18.91	18.80	18.55	18.46	18.50	18.06	18.21	18.07	18.34	23.02	19.61	18.83	18.43	18.24		
3	17 12 02.43	63 40 17.14	0.071	1	21.17	20.67	20.53	20.37	19.77	20.03	19.65	19.58	19.32	19.14	19.60	19.12	18.68	22.61	20.64	19.84	19.49	19.31		
4	17 15 02.65	63 41 03.77	0.086	1	20.32	19.09	18.49	18.26	18.04	17.96	17.71	17.67	17.61	17.47	17.42	17.22	17.02	20.50	18.80	17.96	17.58	17.32		
5	17 12 45.23	63 41 07.68	0.073	1	22.62	20.62	20.52	20.61	20.25	19.98	19.68	19.70	19.74	19.24	19.32	18.94	19.11	21.99	21.13	20.05	19.61	19.22		
6	17 10 01.20	63 40 51.23	0.068	1	19.96	19.36	19.15	18.99	18.71	18.76	18.56	18.50	18.50	18.31	18.44	18.19	17.99	20.81	19.41	18.77	18.45	18.26		
7	17 10 38.30	63 41 00.66	0.087	7	20.55	20.37	20.28	19.92	20.20	20.10	19.83	19.78	19.55	19.56	20.11	20.27	18.94	21.35	20.34	20.04	19.59	19.68		
8	17 10 21.96	63 41 50.38	0.070	1	23.50	20.84	20.61	20.34	20.07	19.71	19.67	19.35	19.71	19.04	19.27	18.85	19.06	21.94	20.94	19.91	19.45	19.07		
9	17 14 05.27	63 42 37.08	0.070	3	19.61	23.45	23.06	21.00	20.47	21.02	20.48	20.81	19.77	20.92	19.90	24.62	19.47	21.93	21.41	20.58	20.26	19.87		
10	17 15 45.57	63 43 12.36	0.088	5	20.48	19.91	19.83	19.92	19.67	19.57	19.52	19.42	19.37	19.45	19.85	19.39	19.83	20.61	19.92	19.50	19.45	19.20		
11	17 11 04.05	63 42 42.99	0.087	4	19.00	18.35	18.19	18.04	17.92	17.83	17.69	17.46	17.55	17.41	17.34	17.43	17.14	19.15	18.31	17.89	17.46	17.32		
12	17 11 49.70	63 43 07.21	0.073	1	20.35	21.60	21.03	20.56	20.27	20.02	19.89	19.83	19.74	19.39	19.50	19.60	19.26	23.42	21.06	20.09	19.66	19.36		
13	17 12 55.68	63 43 40.82	0.081	3	22.13	19.98	19.65	19.45	19.31	19.05	19.01	19.11	18.88	18.83	19.54	19.01	20.01	20.97	19.78	19.14	18.81	18.49		
14	17 14 00.32	63 43 51.35	0.079	2	21.66	20.75	20.35	20.25	20.35	20.02	19.78	19.74	19.73	19.32	19.46	20.00	18.72	22.30	21.11	20.12	19.59	19.43		
15	17 13 10.75	63 44 51.40	0.081	1	19.86	18.71	18.36	18.17	17.96	17.90	17.70	17.63	17.45	17.43	17.45	17.27	17.34	20.14	18.53	17.80	17.54	17.25		
16	17 16 26.83	63 45 13.91	0.083	4	19.65	18.96	18.70	18.47	18.35	18.26	18.10	17.93	17.97	17.85	17.71	17.74	17.57	17.57	20.16	18.88	18.28	17.92	17.67	
17	17 12 52.24	63 44 53.57	0.081	1	19.50	18.26	18.09	17.86	17.51	17.36	17.15	17.04	16.95	16.85	16.85	16.73	16.67	20.51	18.39	17.35	16.94	16.67		
18	17 10 11.50	63 44 29.22	0.079	3	21.03	19.63	19.20	18.98	18.74	18.70	18.53	18.58	18.67	18.06	18.29	18.01	18.28	20.44	19.68	18.92	18.42	18.10		
19	17 10 19.97	63 44 33.25	0.079	1	99.00	19.93	19.49	19.37	18.98	18.85	18.65	18.58	18.59	18.28	18.27	18.24	18.17	21.22	19.99	18.95	18.47	18.08		
20	17 12 07.38	63 45 24.64	0.070	7	21.21	21.21	21.16	20.61	21.47	20.27	20.35	21.48	20.64	20.09	99.00	23.17	18.91	21.68	21.37	20.60	20.43	20.72		
21	17 11 37.76	63 45 21.57	0.079	1	20.34	18.93	18.37	18.15	17.91	17.80	17.59	17.54	17.43	17.28	17.25	17.16	17.12	20.17	18.67	17.80	17.41	17.12		
22	17 10 05.94	63 45 10.71	0.079	3	22.02	20.23	19.83	19.57	19.33	19.40	19.19	18.81	19.15	18.62	18.32	18.68	99.00	21.61	20.18	19.47	19.00	18.89		
23	17 12 28.13	63 45 57.36	0.079	1	19.45	18.58	18.32	18.17	18.00	17.84	17.67	17.61	17.56	17.44	17.34	17.26	17.15	20.22	18.58	17.85	17.53	17.19		
24	17 10 06.21	63 46 02.36	0.087	2	20.22	18.94	18.75	18.44	18.29	18.12	17.94	17.85	17.84	17.64	17.43	17.45	17.21	20.56	19.01	18.16	17.77	17.45		
25	17 09 11.76	63 46 39.15	0.083	2	20.59	20.17	19.83	19.71	19.35	19.13	18.91	18.85	18.84	18.63	18.69	18.62	18.25	21.53	20.15	19.20	18.73	18.36		
26	17 09 02.64	63 47 02.48	0.080	3	18.30	17.53	17.45	17.33	17.01	16.93	16.75	16.63	16.55	16.42	16.37	16.28	16.25	18.80	17.63	16.92	16.54	16.34		
27	17 13 31.33	63 47 58.68	0.083	3	19.25	18.52	18.19	18.06	17.80	17.63	17.47	17.34	17.27	17.14	17.17	17.01	16.82	20.04	18.47	17.65	17.24	16.91		
28	17 12 08.87	63 48 30.92	0.089	2	99.00	20.01	19.51	19.23	19.10	18.99	18.71	18.56	18.44	18.31	18.23	17.90	21.48	18.88	18.93	18.48	17.97			
29	17 12 25.18	63 48 33.40	0.084	3	19.71	18.53	18.34	18.32	18.19	18.09	17.98	17.78	17.82	17.80	18.12	17.70	17.74	19.56	18.47	18.05	17.84	17.69		
30	17 10 20.46	63 48 16.72	0.069	4	19.79	18.91	18.69	18.56	18.46	18.31	18.15	17.93	17.94	17.72	17.79	17.59	17.49	19.92	18.79	18.24	17.99	17.82		
31	17 14 10.07	63 48 57.84	0.084	3	16.13	15.11	14.94	14.86	14.68	14.62	14.53	14.51	14.50	14.47	14.48	14.47	14.47	16.55	15.02	14.62	14.49	14.40		
32	17 16 36.72	63 49 13.78	0.070	3	23.55	22.33	21.75	21.46	20.81	20.75	20.80	19.42	19.07	20.80	20.60	24.62	99.00	21.26	20.80	20.04	19.83	19.61		
33	17 08 43.46	63 48 25.21	0.071	1	22.46	20.60	20.12	20.09	19.84	19.60	19.43	19.47	19.23	19.09	19.05	19.36	19.26	21.59	20.23	19.55	19.29	19.08		
34	17 12 12.86	63 49 14.70	0.087	2	20.04	18.94	18.53	18.27	18.02	17.95	17.68	17.67	17.52	17.46	17.33	17.32	17.10	20.50	18.83	17.93	17.52	17.16		
35	17 13 51.75	63 49 32.87	0.080	3	22.28	20.18	20.33	20.21	19.87	20.12	19.83	20.36	19.93	19.54	20.04	19.94	19.16	21.01	20.26	20.05	20.02	19.71		
36	17 09 53.00	63 49 01.96	0.088	6	21.58	20.72	20.57	20.40	20.41	20.20	20.20	20.09	19.98	19.85	19.90	19.90	20.46	21.17	20.76	20.31	19.88	19.82		
37	17 09 53.33	63 49 07.18	0.077	3	20.44	19.37	19.29	19.17	19.19	19.00	18.92	18.97	18.96	18.72	19.02	18.74	19.12	20.63	19.36	19.11	18.84	18.73		
38	17 13 42.44	63 49 47.54	0.069	2	23.42	19.24	19.02	18.86	18.56	18.51	18.31	18.21	18.09	17.94	18.03	18.00	17.81	20.68	19.24	18.45	18.14	17.80		
39	17 12 35.43	63 49 43.94	0.069	3	99.00	20.21	20.45	20.22	19.44	19.30	19.28	19.01	19.08	18.89	19.64	19.11	19.03	19.43	18.41	22.13	20.61	19.96	19.52	19.07
40	17 13 43.29	63 50 05.75	0.090	7	18.43	17.82	17.68	17.60	17.53	17.51	17.38	16.98	17.39	17.18	17.20	17.21	17.02	18.68	17.82	17.55	17.28	17.15		
41	17 11 26.76	63 50 04.29	0.073	5	21.21	19.97	19.83	19.78	19.83	19.54	19.39	19.32	19.25	19.84	18.90	19.42	18.09	20.87	19.97	19.51	19.27	19.11		
42	17 11 30.26	63 50 31.64	0.073	2	99.00	20.56	19.99	19.78	19.66	19.55	19.45	19.40	19.26	18.89	19.41	18.66	19.31	21.48	20.30	19.59	19.23	19.07		
43	17 14 37.73	63 51 27.89	0.069	1	20.23	19.66	19.37	19.15	18.82	18.68	18.51	18.39	18.29	18.16	18.31	17.95	18.11	21.42	19.46	18.65	18.31	17.99		
44	17 11 45.69	63 51 15.44	0.081	2	20.05	18.80	18.36	18.13																

Table 4—Continued

No. (1)	R.A.(J2000) (2)	Decl. (3)	z_{phot} (4)	T (5)	b (6)	d (7)	e (8)	f (9)	g (10)	h (11)	i (12)	j (13)	k (14)	m (15)	n (16)	σ (17)	p (18)	u' (19)	g' (20)	r' (21)	i' (22)	z' (23)
54	17 15 07.13	63 53 03.14	0.070	3	99.00	20.89	21.33	20.60	19.91	20.15	19.74	20.55	19.63	19.12	21.02	24.18	99.00	21.51	21.02	20.12	19.72	19.36
55	17 15 00.38	63 53 37.99	0.071	4	20.46	19.79	19.39	19.29	19.03	18.92	18.75	18.75	18.55	18.45	18.53	18.26	18.34	20.58	19.45	18.85	18.62	18.28
56	17 16 07.49	63 53 49.77	0.077	2	20.03	19.93	19.37	19.02	18.76	18.62	18.44	18.38	18.34	18.11	17.93	18.00	17.45	20.61	19.60	18.64	18.30	17.91
57	17 15 22.27	63 53 50.65	0.083	6	20.17	19.41	19.49	19.39	19.13	19.37	19.05	19.05	18.90	18.84	18.73	19.16	18.69	20.52	19.59	19.27	18.97	18.70
58	17 13 01.88	63 53 43.31	0.079	2	19.53	18.88	18.41	18.20	17.99	17.88	17.65	17.59	17.46	17.30	17.14	17.06	16.99	20.21	18.66	17.83	17.49	17.20
59	17 13 24.38	63 54 03.30	0.071	1	99.00	20.66	19.99	19.79	19.51	19.28	19.12	18.95	18.84	18.67	18.78	18.80	18.59	21.63	20.08	19.24	18.87	18.72
60	17 16 04.89	63 54 33.55	0.087	3	19.00	18.37	18.15	18.08	17.98	17.87	17.74	17.76	17.73	17.66	17.67	17.61	17.47	19.19	18.20	17.86	17.73	17.57
61	17 11 15.84	63 54 03.81	0.083	1	20.79	20.01	19.03	18.60	18.56	18.45	18.13	18.09	18.02	17.85	17.64	17.76	17.52	21.58	19.50	18.44	17.99	17.61
62	17 11 16.66	63 54 28.17	0.087	2	19.63	18.62	18.29	18.05	17.82	17.73	17.50	17.48	17.34	17.26	17.17	17.19	17.19	20.06	18.49	17.71	17.34	17.01
63	17 11 19.79	63 54 28.67	0.078	3	19.71	18.74	18.45	18.25	18.02	17.91	17.75	17.75	17.59	17.44	17.56	17.45	17.12	20.24	18.69	17.92	17.58	17.29
64	17 12 45.76	63 54 52.68	0.071	1	20.39	19.29	19.01	18.77	18.62	18.52	18.29	18.32	18.16	17.99	17.89	17.85	17.80	20.99	19.26	18.48	18.18	17.94
65	17 13 07.62	63 54 58.11	0.083	1	19.88	19.10	18.44	18.24	18.00	17.88	17.69	17.57	17.54	17.43	17.48	17.17	17.20	20.42	18.72	17.86	17.52	17.21
66	17 12 45.33	63 55 04.89	0.070	1	19.45	18.91	18.41	18.22	17.95	17.87	17.70	17.64	17.60	17.42	17.54	17.32	17.42	20.48	18.73	17.89	17.56	17.33
67	17 16 07.38	63 55 28.68	0.083	4	19.05	18.64	18.34	18.25	18.02	17.92	17.76	17.70	17.68	17.49	17.44	17.41	17.28	19.63	18.59	17.98	17.60	17.42
68	17 11 05.72	63 54 50.16	0.081	2	19.59	18.99	18.61	18.33	18.06	18.01	17.77	17.70	17.57	17.46	17.40	17.31	17.15	20.36	18.90	18.00	17.56	17.22
69	17 14 43.90	63 55 30.01	0.089	1	20.82	19.57	19.29	19.10	18.87	18.63	18.46	18.28	18.31	18.29	17.93	18.17	17.94	21.14	19.49	18.64	18.27	18.00
70	17 13 03.63	63 55 25.52	0.068	3	21.45	19.73	19.83	19.80	19.50	19.35	19.34	19.18	19.20	19.09	19.45	19.19	19.79	21.59	20.16	19.38	19.17	18.98
71	17 13 25.29	63 55 29.02	0.084	1	20.65	20.35	20.08	19.96	19.90	19.51	19.49	19.47	19.47	19.34	19.86	18.82	18.83	21.13	20.92	19.65	19.32	19.07
72	17 11 50.11	63 55 24.66	0.073	1	20.16	20.00	19.46	19.28	18.95	18.85	18.63	18.51	18.70	18.41	18.34	18.48	18.09	21.79	19.78	18.94	18.56	18.23
73	17 13 12.76	63 55 39.88	0.090	1	19.74	18.45	17.90	17.57	17.41	17.21	16.95	16.90	16.80	16.70	16.55	16.48	16.39	20.12	18.15	17.17	16.81	16.50
74	17 10 58.43	63 55 19.71	0.083	4	21.41	19.23	19.08	19.02	18.76	18.67	18.52	18.47	18.41	18.37	18.47	18.10	18.05	20.05	19.19	18.67	18.39	18.17
75	17 13 37.09	63 55 46.96	0.088	2	18.72	20.54	19.97	19.80	19.81	19.62	19.47	19.30	19.26	19.23	19.50	18.92	19.47	21.93	20.41	19.62	19.24	19.00
76	17 14 30.98	63 55 58.80	0.090	1	19.41	19.74	19.40	19.17	19.08	18.76	18.64	18.37	18.00	18.31	17.86	21.45	19.64	18.78	18.42	18.13		
77	17 16 01.30	63 56 46.24	0.078	3	20.33	19.60	19.33	19.37	19.10	19.11	19.01	18.84	18.86	18.76	19.78	19.31	19.49	20.66	19.56	19.11	18.84	18.94
78	17 12 47.18	63 56 24.97	0.079	1	19.77	18.89	18.39	18.25	18.00	17.96	17.74	17.66	17.57	17.47	17.32	17.44	17.15	20.42	18.73	17.93	17.58	17.30
79	17 15 26.20	63 56 57.27	0.079	1	20.17	19.19	18.88	18.78	18.42	18.31	18.08	18.11	17.97	17.70	17.69	17.78	17.61	21.02	19.19	18.33	17.93	17.68
80	17 11 11.81	63 56 39.46	0.079	1	99.00	19.97	20.01	19.67	19.51	19.29	19.03	19.15	18.90	18.62	18.95	19.01	18.42	22.59	20.18	19.25	18.93	18.57
81	17 12 37.16	63 56 58.79	0.080	1	19.42	18.67	18.23	17.98	17.71	17.61	17.37	17.26	17.18	17.06	16.93	16.89	16.69	20.27	18.44	17.56	17.21	16.89
82	17 13 24.42	63 57 09.33	0.071	1	19.96	19.16	18.73	18.40	18.15	18.07	17.87	17.73	17.67	17.47	17.41	17.31	17.31	20.77	18.93	18.04	17.67	17.37
83	17 10 53.65	63 56 54.69	0.083	1	19.76	19.40	18.84	18.56	18.42	18.42	18.19	18.19	17.97	18.01	18.06	17.78	17.59	20.66	19.26	18.36	18.02	17.69
84	17 13 19.17	63 57 25.70	0.082	1	20.89	19.38	18.96	18.70	18.44	18.36	18.15	18.09	17.99	17.92	17.95	17.79	17.46	21.05	19.22	18.35	17.98	17.64
85	17 12 16.17	63 57 19.89	0.089	2	20.10	19.57	19.16	18.85	18.66	18.49	18.30	18.28	18.03	17.97	17.76	17.87	17.75	21.06	19.32	18.47	18.06	17.74
86	17 10 21.34	63 56 59.96	0.082	1	22.88	24.32	21.48	21.69	21.16	21.75	20.93	20.89	20.39	21.97	19.71	99.00	20.63	23.80	21.35	21.08	21.00	22.28
87	17 12 31.78	63 57 29.56	0.076	1	20.69	19.41	18.70	18.57	18.29	18.19	17.97	17.89	17.76	17.66	17.63	17.34	20.71	19.07	18.19	17.84	17.57	
88	17 10 39.72	63 57 11.79	0.071	3	20.12	21.06	20.88	20.27	20.03	19.79	19.72	19.52	19.81	19.05	19.92	19.59	18.87	23.27	20.68	19.95	19.60	19.21
89	17 13 28.42	63 57 49.48	0.079	1	21.92	19.92	19.39	19.15	19.03	18.83	18.62	18.52	18.34	18.47	18.04	18.50	21.72	19.68	18.82	18.50	18.16	
90	17 14 27.80	63 57 59.70	0.068	1	99.00	20.20	19.86	19.72	19.43	19.39	19.23	19.53	19.68	18.87	18.83	18.52	18.67	21.66	20.37	19.61	19.41	18.84
91	17 13 13.39	63 57 53.75	0.079	1	99.00	21.92	20.67	20.49	19.96	20.62	20.24	19.79	19.93	20.34	19.51	21.62	99.00	25.28	21.48	20.41	20.06	19.73
92	17 08 38.25	63 56 59.41	0.068	1	19.68	18.91	18.60	18.46	18.14	18.01	17.87	17.79	17.84	17.45	17.51	17.34	17.22	20.64	18.97	18.08	17.74	
93	17 12 15.43	63 57 47.67	0.087	3	99.00	20.89	21.06	20.68	20.37	20.64	19.93	19.76	19.65	19.65	99.00	19.48	19.34	24.32	21.04	20.28	19.91	19.79
94	17 14 16.42	63 58 24.08	0.088	1	22.06	20.08	19.65	19.41	19.14	19.06	18.77	18.70	18.61	18.61	18.09	18.31	18.45	21.93	19.85	18.99	18.65	18.31
95	17 12 15.72	63 58 32.82	0.090	2	20.80	20.38	19.99	19.56	19.69	19.26	19.17	18.86	19.02	18.77	18.66	19.50	18.06	21.81	20.12	19.31	18.93	18.65
96	17 13 36.84	63 58 48.67	0.090	1	20.78	19.56	19.26	19.08	18.90	18.75	18.54	18.58	18.50	18.36	18.35	17.84	21.62	19.49	18.79	18.44	18.23	
97	17 11 56.81	63 58 46.67	0.088	3	99.00	21.04	20.74	20.67	20.68	20.20	19.93	19.68	19.91	19.47	19.93	19.37	2					

Table 4—Continued

No. (1)	R.A.(J2000) (2)	Decl. (3)	z_{phot} (4)	T (5)	b (6)	d (7)	e (8)	f (9)	g (10)	h (11)	i (12)	j (13)	k (14)	m (15)	n (16)	σ (17)	p (18)	u' (19)	g' (20)	r' (21)	i' (22)	z' (23)
107	17 13 20.91	64 00 09.50	0.072	1	21.22	19.64	19.34	19.19	18.94	18.88	18.65	18.62	18.37	18.33	18.34	18.49	18.05	21.14	19.56	18.78	18.47	18.23
108	17 13 27.20	64 00 12.96	0.079	4	20.66	19.64	19.42	19.24	19.13	19.01	18.80	18.90	18.68	18.49	18.76	18.39	18.93	20.69	19.58	19.01	18.68	18.39
109	17 12 23.44	64 00 05.16	0.081	1	19.92	18.84	18.36	18.19	18.00	17.84	17.62	17.55	17.47	17.36	17.25	17.15	16.99	20.54	18.72	17.83	17.46	17.16
110	17 13 32.86	64 00 16.84	0.083	1	20.31	18.81	18.34	18.00	17.80	17.71	17.45	17.38	17.25	17.14	17.08	17.06	17.05	20.67	18.54	17.67	17.26	16.94
111	17 11 42.46	64 00 05.11	0.079	1	19.59	18.47	18.32	18.10	17.90	17.74	17.57	17.51	17.43	17.32	17.16	17.19	16.99	20.37	18.59	17.77	17.39	17.07
112	17 12 28.09	64 00 12.63	0.077	1	20.08	18.75	18.39	18.28	17.96	17.92	17.65	17.53	17.47	17.34	17.25	17.22	17.44	20.58	18.74	17.86	17.49	17.18
113	17 12 44.22	64 00 34.11	0.079	2	21.14	19.71	19.10	18.90	99.00	18.47	18.27	18.25	18.22	17.99	18.16	17.98	17.69	21.10	19.34	18.51	18.15	17.83
114	17 11 17.57	64 00 25.49	0.072	3	21.28	20.36	19.92	19.79	19.40	19.27	19.22	19.04	19.02	18.94	19.61	18.97	19.02	21.23	20.08	19.31	18.97	18.67
115	17 13 02.74	64 00 50.95	0.079	1	21.14	20.38	20.15	19.84	19.99	19.74	19.46	19.62	20.81	19.71	99.00	20.11	17.93	21.99	20.64	20.30	20.05	19.79
116	17 13 11.24	64 00 55.76	0.081	1	20.05	18.99	18.53	18.24	17.99	17.84	17.58	17.51	17.38	17.26	17.16	17.06	16.88	20.70	18.81	17.83	17.37	16.97
117	17 12 22.13	64 00 49.08	0.080	2	22.15	20.33	19.73	19.48	19.38	19.20	18.92	18.82	18.56	18.46	18.72	18.43	18.15	21.39	19.90	19.07	18.68	18.35
118	17 12 23.93	64 00 54.90	0.087	1	20.96	20.04	19.82	19.52	19.44	19.23	18.94	18.94	18.79	18.60	18.44	18.52	18.55	21.89	20.02	19.18	18.81	18.52
119	17 12 56.41	64 01 02.35	0.070	1	19.94	19.17	18.69	18.52	18.23	18.16	17.92	17.88	17.69	17.61	17.56	17.39	20.71	18.97	18.09	17.74	17.42	
120	17 13 51.97	64 01 16.57	0.090	1	99.00	19.94	19.51	19.38	19.17	19.00	18.78	18.80	18.65	18.62	18.59	18.48	18.67	21.62	19.79	19.00	18.64	18.44
121	17 12 43.45	64 01 07.84	0.078	1	20.04	19.88	18.65	18.57	18.59	18.64	18.33	18.41	99.00	18.34	18.09	18.25	18.06	21.13	19.48	18.67	18.31	18.02
122	17 11 58.36	64 01 04.30	0.068	2	19.45	18.58	18.18	17.96	17.74	17.62	17.41	17.30	17.24	17.06	16.98	16.85	16.90	20.08	18.49	17.61	17.23	16.88
123	17 12 53.90	64 01 13.31	0.079	1	20.48	19.21	18.76	18.54	18.19	18.14	17.79	17.72	17.57	17.42	17.45	17.22	20.95	19.11	18.07	17.60	17.22	
124	17 11 01.28	64 01 05.31	0.088	2	19.63	18.57	18.07	17.80	17.59	17.41	17.23	17.13	17.07	16.98	16.92	16.70	16.59	19.92	18.29	17.40	17.06	16.71
125	17 13 08.85	64 01 37.31	0.079	1	19.13	18.57	18.07	17.81	17.55	17.40	17.20	17.13	17.07	16.91	16.83	16.77	16.63	20.32	18.35	17.42	17.03	16.70
126	17 15 04.52	64 02 02.63	0.083	2	19.66	19.22	18.75	18.51	18.25	18.11	17.84	17.81	17.71	17.52	17.53	17.33	17.11	20.58	18.96	18.13	17.66	17.35
127	17 12 45.10	64 01 51.70	0.068	1	21.66	19.50	18.86	18.62	18.35	18.17	18.01	17.97	17.95	17.68	17.69	17.50	99.00	20.85	19.12	18.25	17.85	17.55
128	17 13 07.40	64 01 54.92	0.071	1	17.92	16.85	16.61	16.58	16.34	16.23	16.06	16.06	15.93	15.86	15.84	15.80	15.77	18.22	16.81	16.20	15.95	15.81
129	17 13 23.09	64 02 00.60	0.083	1	19.84	19.17	18.70	18.42	18.09	18.05	17.81	17.78	17.72	17.53	17.37	17.36	17.31	20.82	18.96	18.07	17.67	17.40
130	17 12 13.29	64 01 57.77	0.068	1	19.30	18.31	17.84	17.66	17.39	17.35	17.11	17.04	16.94	16.85	16.79	16.73	16.56	19.69	18.22	17.29	16.98	16.68
131	17 15 10.18	64 02 26.94	0.068	1	19.22	18.47	17.92	17.71	17.48	17.38	17.12	17.08	17.06	16.84	16.91	16.67	16.65	20.11	18.23	17.40	17.00	16.71
132	17 16 05.95	64 02 32.96	0.083	1	19.86	18.94	18.33	18.11	17.89	17.85	17.56	17.55	17.41	17.29	17.16	17.19	16.96	20.31	18.70	17.81	17.43	17.16
133	17 12 07.93	64 02 06.81	0.083	1	20.90	20.49	19.80	19.50	19.53	19.26	19.06	19.16	19.23	19.26	18.98	18.90	18.73	22.51	20.27	19.46	18.98	18.89
134	17 13 27.93	64 02 19.14	0.083	1	20.19	19.46	18.95	18.73	18.58	18.41	18.16	18.18	18.03	17.86	17.90	17.93	17.65	21.57	19.39	18.44	17.98	17.67
135	17 11 39.03	64 02 04.91	0.090	1	19.66	18.73	18.46	18.34	18.11	17.97	17.77	17.68	17.60	17.55	17.47	17.35	17.36	20.24	18.70	17.96	17.60	17.32
136	17 12 48.34	64 02 19.20	0.075	1	21.37	21.46	21.39	21.00	21.33	20.60	20.54	20.11	20.44	19.89	21.23	21.04	99.00	24.07	21.46	20.67	20.31	20.09
137	17 16 24.56	64 02 44.05	0.070	3	99.00	20.59	20.37	20.61	20.17	20.65	20.35	19.79	20.27	21.69	19.35	24.00	99.00	22.22	21.42	20.51	20.29	20.01
138	17 14 35.63	64 02 36.39	0.080	2	20.56	20.43	19.95	19.90	19.84	19.60	19.26	19.44	19.34	19.03	20.60	19.53	19.14	21.98	20.35	19.64	19.26	18.94
139	17 11 37.14	64 02 19.20	0.083	3	20.21	19.14	18.75	18.60	18.33	18.21	17.99	17.87	17.80	17.64	17.68	17.44	17.43	20.39	18.95	18.18	17.81	17.54
140	17 12 07.78	64 02 34.61	0.079	1	20.07	19.83	18.84	18.70	18.77	18.70	18.52	18.53	18.43	18.40	18.00	18.18	18.07	21.66	19.78	18.73	18.39	17.87
141	17 12 33.92	64 02 46.44	0.088	1	21.23	19.53	19.01	18.70	18.58	18.45	18.17	18.13	18.11	17.98	18.02	17.70	17.75	21.35	19.36	18.45	18.07	17.81
142	17 11 49.04	64 02 48.20	0.068	1	20.54	19.52	19.22	18.93	18.71	18.60	18.42	18.39	18.56	18.05	17.85	18.08	18.18	21.39	19.57	18.74	18.36	18.02
143	17 09 49.60	64 02 31.20	0.082	3	25.35	21.12	22.41	21.57	20.65	20.40	20.58	20.91	20.42	21.71	20.47	23.88	20.29	21.91	21.33	20.48	20.44	20.45
144	17 13 35.38	64 03 12.10	0.079	1	20.77	19.81	19.26	19.00	18.69	18.75	18.41	18.54	18.56	18.31	18.18	18.05	17.98	21.55	19.68	18.83	18.42	18.22
145	17 13 09.58	64 03 12.23	0.081	1	20.21	19.19	18.67	18.35	18.21	18.04	17.77	17.73	17.58	17.44	17.56	17.28	17.23	20.71	18.96	17.99	17.61	17.29
146	17 15 04.88	64 03 27.94	0.068	1	20.39	20.35	19.66	19.27	18.92	18.91	18.60	18.78	18.86	18.42	18.69	18.44	18.02	21.93	19.87	19.05	18.67	18.32
147	17 12 54.34	64 03 16.98	0.080	1	21.52	19.60	18.96	18.75	18.55	18.38	18.14	18.16	17.98	17.78	18.22	20.95	19.28	18.43	18.08	17.76	17.76	
148	17 12 21.75	64 03 12.51	0.071	2	21.17	20.25	19.62	19.42	18.98	18.93	18.64	18.62	18.47	18.40	18.67	18.43	18.44	21.77	19.76	18.87	18.50	18.11
149	17 13 23.80	64 03 23.08	0.078	1	20.51	20.66	19.83	19.69	19.36	19.33	18.82	19.01	18.93	18.69	18.80	18.58	20.92	22.08	20.12	19.27	18.93	18.70
150	17 09 07.71	64 02 34.44	0.090	4	19.82	19.07	18.93	18.74	18.63	18.5												

Table 4—Continued

No. (1)	R.A.(J2000) (2)	Decl. (3)	z_{phot} (4)	T (5)	b (6)	d (7)	e (8)	f (9)	g (10)	h (11)	i (12)	j (13)	k (14)	m (15)	n (16)	σ (17)	p (18)	u' (19)	g' (20)	r' (21)	i' (22)	z' (23)	
160	17 12 08.19	64 03 48.71	0.080	5	22.11	20.62	20.73	20.62	20.25	20.16	20.06	20.69	20.07	20.00	22.53	20.34	99.00	21.43	20.61	20.27	20.03	19.87	
161	17 13 10.00	64 04 03.84	0.068	1	20.92	19.65	18.87	18.75	18.50	18.47	18.15	18.12	18.09	17.81	17.81	17.68	18.25	20.97	19.36	18.43	18.08	17.78	
162	17 12 09.40	64 03 59.06	0.082	1	21.54	19.09	18.66	18.48	18.24	18.08	17.87	17.81	17.74	17.62	17.66	17.45	17.24	20.92	18.96	18.09	17.71	17.38	
163	17 12 40.87	64 04 15.38	0.084	1	19.89	18.71	18.05	17.82	17.53	17.44	17.23	17.13	17.04	16.88	16.86	16.69	16.67	20.06	18.67	17.43	17.02	16.70	
164	17 12 10.41	64 04 13.15	0.083	1	19.81	18.80	18.29	18.05	17.84	17.75	17.53	17.48	17.47	17.26	17.17	17.14	16.96	21.03	18.67	17.79	17.39	17.09	
165	17 13 38.80	64 04 29.74	0.069	1	23.00	20.67	19.87	19.72	19.37	19.33	19.18	18.98	19.08	18.89	19.67	18.66	18.48	22.27	20.14	19.35	19.02	18.75	
166	17 13 18.08	64 04 29.49	0.086	1	19.85	18.96	18.43	18.13	17.93	17.84	17.55	17.52	17.43	17.31	17.15	17.16	17.00	20.14	18.78	17.85	17.39	17.22	
167	17 12 46.40	64 04 31.91	0.077	1	21.97	18.99	18.76	18.67	18.41	18.38	18.14	18.19	18.12	18.04	17.99	18.00	17.99	20.18	18.89	18.36	18.11	17.94	
168	17 10 12.56	64 04 04.69	0.068	1	23.08	20.02	19.48	19.40	19.17	19.08	18.86	18.81	18.81	18.58	18.28	18.35	18.74	22.16	19.86	19.10	18.75	18.45	
169	17 10 04.45	64 04 05.02	0.068	2	20.91	20.57	20.20	20.27	19.91	19.73	19.66	19.58	19.72	19.29	19.72	19.56	19.48	21.86	20.67	19.89	19.52	19.13	
170	17 12 51.27	64 04 37.40	0.079	1	20.30	19.52	18.93	18.70	18.50	18.39	18.19	18.13	18.04	17.97	17.77	17.86	17.67	21.17	19.22	18.39	18.03	17.76	
171	17 12 47.94	64 04 38.56	0.080	1	21.18	19.83	19.52	19.58	19.41	19.23	19.16	19.30	19.03	18.92	19.88	19.03	18.95	20.98	19.71	19.22	19.06	19.25	
172	17 12 40.34	64 04 43.06	0.083	1	19.50	18.32	17.85	17.66	17.49	17.40	17.17	17.18	17.14	17.02	16.93	16.86	16.91	19.65	18.14	17.41	17.10	16.86	
173	17 11 34.10	64 04 33.64	0.078	1	19.80	18.39	18.03	17.78	17.53	17.39	17.19	17.08	17.07	16.86	16.81	16.67	16.62	20.21	18.34	17.41	17.03	16.71	
174	17 12 19.48	64 04 42.60	0.083	2	20.16	19.18	18.74	18.50	18.20	18.13	17.91	17.84	17.69	17.64	17.51	17.37	17.70	20.84	19.05	18.11	17.70	17.33	
175	17 10 17.20	64 04 25.35	0.083	3	20.41	19.55	19.36	19.10	18.97	18.80	18.56	18.61	18.52	18.45	18.45	18.00	21.50	19.76	18.98	18.57	18.33		
176	17 13 55.37	64 05 05.26	0.080	1	19.53	18.76	18.34	18.17	17.99	17.77	17.59	17.58	17.46	17.34	17.31	17.23	17.18	20.22	18.57	17.76	17.45	17.16	
177	17 12 28.53	64 04 56.00	0.079	1	20.04	19.39	18.88	18.59	18.41	18.22	18.01	17.98	17.91	17.66	17.62	17.65	17.51	20.98	19.11	18.25	17.86	17.61	
178	17 12 44.49	64 04 58.28	0.070	1	20.99	19.64	18.99	18.76	18.53	18.37	18.08	18.02	18.13	17.83	17.80	17.90	18.01	21.27	19.35	18.42	18.03	17.69	
179	17 12 12.75	64 04 55.42	0.068	1	20.54	19.53	19.14	19.04	18.67	18.64	18.45	18.46	18.23	18.10	18.05	17.98	18.14	20.98	19.38	18.59	18.28	18.06	
180	17 12 30.89	64 05 05.23	0.079	1	20.46	19.02	18.70	18.40	18.23	18.10	17.90	17.90	17.75	17.68	17.60	17.66	17.23	20.59	18.85	18.09	17.75	17.48	
181	17 14 20.14	64 05 30.36	0.090	1	20.08	19.28	18.81	18.51	18.31	18.16	17.96	17.91	17.82	17.71	17.50	17.38	20.60	19.04	18.16	17.80	17.49		
182	17 12 37.91	64 05 19.62	0.081	1	19.24	18.48	18.03	17.78	17.56	17.41	17.20	17.10	16.98	16.87	16.93	16.73	16.67	20.03	18.27	17.38	17.00	16.70	
183	17 12 17.19	64 05 19.43	0.078	1	20.32	19.68	19.66	19.48	19.15	19.06	18.93	18.99	18.85	18.61	18.41	18.56	18.12	21.47	19.95	19.14	18.77	18.57	
184	17 12 06.51	64 05 20.44	0.079	2	19.87	18.81	18.40	18.24	17.82	17.83	17.59	17.56	17.47	17.36	17.36	17.13	16.94	20.56	18.71	17.83	17.44	17.10	
185	17 12 52.15	64 05 32.17	0.069	1	22.24	19.49	19.16	19.00	18.60	18.55	18.31	18.22	18.10	18.05	17.95	17.83	17.57	21.33	19.38	18.49	18.14	17.83	
186	17 14 00.35	64 05 42.14	0.079	1	17.79	19.05	18.70	18.52	18.30	18.16	17.98	17.92	17.82	17.70	17.61	17.54	17.55	20.85	19.05	18.18	17.78	17.38	
187	17 14 28.17	64 05 46.40	0.068	2	20.35	18.84	18.47	18.33	18.01	17.79	17.67	17.61	17.54	17.35	17.45	17.25	17.11	20.26	18.70	17.85	17.47	17.12	
188	17 11 36.17	64 05 27.47	0.069	3	23.71	21.60	22.09	21.05	21.41	20.63	20.39	20.62	20.39	20.53	19.74	20.33	19.88	19.99	24.72	21.36	20.72	20.43	
189	17 12 29.09	64 05 47.58	0.079	1	19.75	19.05	18.62	18.43	18.11	18.05	17.79	17.73	17.69	17.55	17.50	17.32	17.52	20.81	18.93	18.04	17.66	17.35	
190	17 13 09.29	64 05 55.63	0.083	1	21.33	19.39	18.96	18.74	18.55	18.43	18.19	18.19	18.08	17.97	17.90	17.96	17.62	20.92	19.21	18.43	18.06	17.78	
191	17 10 33.33	64 05 31.48	0.073	2	23.05	21.88	20.56	20.20	19.92	19.76	19.64	19.67	19.95	19.43	19.15	19.63	19.94	21.48	20.87	20.05	19.61	19.12	
192	17 13 30.89	64 06 05.02	0.073	7	18.96	18.70	18.35	18.33	18.24	18.15	18.33	18.11	18.04	18.08	18.12	17.61	19.59	18.66	18.30	18.07	18.00		
193	17 14 51.49	64 06 32.13	0.090	3	29.00	20.18	19.94	19.75	19.54	19.44	19.30	19.12	19.14	18.86	18.82	18.44	18.71	18.31	21.30	20.07	19.29	18.89	18.66
194	17 16 22.64	64 06 48.03	0.071	2	19.84	19.14	18.73	18.63	18.41	18.33	18.12	18.05	17.95	17.77	17.91	17.76	17.75	20.17	18.87	18.26	18.01	17.87	
195	17 15 48.31	64 06 52.01	0.068	3	20.53	19.97	19.50	19.09	18.87	18.75	18.58	18.75	18.55	18.32	18.24	18.25	18.08	21.24	19.78	18.97	18.61	18.20	
196	17 14 52.86	64 06 49.32	0.079	2	19.46	18.78	18.31	18.07	17.83	17.72	17.50	17.47	17.31	17.16	17.08	17.13	16.84	20.01	18.58	17.71	17.31	17.01	
197	17 15 16.81	64 06 58.36	0.083	3	18.52	19.68	18.28	18.21	18.02	18.50	18.33	18.71	21.71	18.66	17.85	17.85	19.75	17.40	22.58	20.82	20.15	19.63	19.62
198	17 12 15.35	64 06 58.25	0.076	3	20.62	18.97	18.77	18.72	18.59	18.49	18.42	18.30	18.35	18.17	18.32	18.07	18.35	20.08	18.91	18.48	18.34	18.26	
199	17 16 05.77	64 07 29.23	0.078	1	20.77	19.31	18.79	18.60	18.29	18.24	18.08	17.98	17.90	17.71	17.58	17.68	17.27	20.62	19.03	18.21	17.91	17.64	
200	17 13 40.76	64 07 30.16	0.083	3	20.94	19.66	19.47	19.24	19.18	19.32	18.90	18.72	19.10	18.79	18.59	19.31	20.17	21.04	19.67	19.27	19.03	19.05	
201	17 14 20.63	64 07 36.04	0.068	1	21.19	19.68	19.06	18.85	18.58	18.42	18.26	18.25	18.20	17.99	17.92	17.98	17.59	20.90	19.34	18.49	18.11	17.78	
202	17 14 36.43	64 07 49.23	0.077	1	99.00	21.08	21.37	20.74	20.32	21.05	20.12	20.15	20.00	19.59	20.19	20.41	99.00	24.42	21.34	20.58	20.34	20.14	
203	17 13 27.98	64 07 43.51	0.083	3	19.62	18.77	18.62	18.54	18.39	18.27	18.10	18.02	18.12	17.89	17.86	17.81	17.64	19.89	18.81	18.33	18.03		

Table 4—Continued

No. (1)	R.A.(J2000) (2)	Decl. (3)	z_{phot} (4)	T (5)	b (6)	d (7)	e (8)	f (9)	g (10)	h (11)	i (12)	j (13)	k (14)	m (15)	n (16)	σ (17)	p (18)	u' (19)	g' (20)	r' (21)	i' (22)	z' (23)	
213	17 11 14.64	64 08 22.73	0.077	2	19.87	19.62	19.05	18.92	18.73	18.53	18.31	18.24	18.20	18.02	18.14	17.79	17.82	21.17	19.36	18.55	18.15	17.82	
214	17 11 25.03	64 08 34.05	0.071	3	99.00	21.11	20.42	20.18	20.73	19.69	19.54	19.69	19.16	20.05	19.50	18.98	22.16	20.50	19.90	19.56	19.29		
215	17 10 37.83	64 08 35.95	0.083	1	19.93	19.44	19.04	18.85	18.69	18.64	18.46	18.42	18.37	18.34	18.22	18.16	17.52	21.08	19.46	18.68	18.31	18.03	
216	17 11 43.41	64 08 47.98	0.077	1	20.14	19.20	18.92	18.70	18.47	18.34	18.15	18.06	18.11	17.90	17.96	17.73	17.58	20.75	19.14	18.38	18.04	17.76	
217	17 12 09.79	64 09 04.67	0.083	1	20.85	20.24	19.57	19.47	19.29	19.23	18.95	18.81	18.69	18.85	18.72	18.59	18.52	21.88	19.90	19.12	18.77	18.48	
218	17 13 19.03	64 09 15.36	0.075	1	99.00	20.34	19.71	19.55	19.30	19.26	18.99	19.07	18.82	18.81	18.52	18.94	19.15	21.96	20.04	19.21	18.86	18.63	
219	17 14 30.09	64 09 31.95	0.072	1	22.73	20.35	19.74	19.51	19.08	19.37	19.13	18.93	18.97	18.68	19.29	18.58	18.55	22.48	20.41	19.34	18.96	18.66	
220	17 15 05.51	64 09 38.46	0.083	3	20.52	20.39	20.34	20.10	19.87	19.93	19.60	19.42	19.48	19.27	19.51	19.16	20.76	22.14	20.50	19.86	19.49	19.29	
221	17 14 09.35	64 09 48.26	0.081	2	19.61	19.31	18.83	18.51	18.34	18.18	17.95	17.83	17.73	17.57	17.45	17.39	17.26	21.00	19.08	18.15	17.73	17.42	
222	17 12 54.03	64 09 54.88	0.071	3	20.16	19.65	19.38	19.42	19.28	19.15	19.14	19.16	19.01	19.00	18.83	19.29	18.49	20.44	19.48	19.17	19.01	19.07	
223	17 09 14.64	64 09 14.29	0.073	3	20.74	20.68	19.95	19.77	19.59	19.42	19.30	19.25	19.27	18.82	18.95	19.82	19.39	20.79	20.24	19.52	19.15	18.73	
224	17 14 33.87	64 10 14.85	0.071	2	20.65	21.72	20.06	19.94	19.72	19.58	19.31	19.33	19.33	19.00	19.20	18.80	19.67	22.23	20.34	19.62	19.25	19.01	
225	17 14 06.11	64 10 19.88	0.089	2	18.60	19.27	19.01	18.88	18.60	18.38	18.15	18.17	18.09	17.95	17.85	17.69	17.80	20.73	19.39	18.47	17.98	17.63	
226	17 12 57.56	64 10 28.17	0.087	7	20.31	19.01	18.90	18.75	18.73	18.56	18.45	18.42	18.34	18.21	18.46	18.07	18.18	19.98	19.00	18.58	18.31	18.13	
227	17 15 05.25	64 10 57.15	0.083	1	19.95	19.15	18.64	18.45	18.14	18.08	17.86	17.82	17.59	17.61	17.48	17.44	17.27	20.54	18.89	18.03	17.64	17.42	
228	17 15 58.32	64 11 01.71	0.088	1	20.75	19.83	19.59	19.35	19.08	18.94	18.73	18.70	18.56	18.58	18.34	18.53	18.41	21.68	20.08	18.96	18.53	18.29	
229	17 14 43.44	64 11 04.43	0.083	3	20.56	19.57	19.57	19.50	19.23	19.08	19.11	19.07	19.05	18.94	18.68	20.05	19.50	20.84	19.62	19.20	18.93	18.79	
230	17 14 41.77	64 11 17.83	0.079	1	99.00	20.34	20.06	19.78	19.48	19.48	19.17	19.51	19.06	18.94	19.73	19.68	19.07	21.78	20.11	19.44	19.11	18.78	
231	17 10 27.99	64 10 39.27	0.079	3	99.00	20.08	19.75	19.53	19.21	19.33	18.93	18.86	18.70	18.47	18.65	18.31	18.19	22.09	19.92	19.19	18.80	18.52	
232	17 14 00.17	64 11 21.81	0.083	1	16.26	19.11	18.57	18.31	18.15	17.93	17.76	17.65	17.61	17.43	17.43	17.29	17.29	20.40	18.80	17.94	17.58	17.31	
233	17 12 35.36	64 11 10.63	0.086	2	20.32	18.92	18.65	18.35	18.10	17.93	17.76	17.63	17.49	17.42	17.33	17.28	17.37	20.39	18.83	17.91	17.50	17.21	
234	17 16 16.42	64 11 45.02	0.073	1	99.00	19.23	19.01	18.84	18.48	18.46	18.26	18.21	18.17	17.95	17.90	18.14	18.37	20.99	19.30	18.49	18.12	17.86	
235	17 13 05.04	64 11 48.62	0.078	2	20.42	19.54	19.32	19.15	18.89	18.74	18.64	18.71	18.48	18.36	18.20	18.37	18.25	20.84	19.58	18.81	18.42	18.24	
236	17 11 57.30	64 11 42.33	0.072	1	20.52	20.22	19.56	19.34	19.03	19.07	18.89	18.77	18.69	18.65	18.38	18.75	18.23	21.28	19.82	19.00	18.74	18.43	
237	17 13 25.49	64 12 12.62	0.086	1	20.34	19.48	19.11	18.97	18.75	18.68	18.55	18.47	18.54	18.34	18.28	18.25	18.45	21.10	19.52	18.78	18.40	18.21	
238	17 13 26.42	64 12 24.27	0.090	2	20.26	19.31	18.80	18.53	18.32	18.24	18.09	18.15	18.00	17.84	17.67	17.65	17.46	20.85	19.32	18.44	17.88	17.56	
239	17 12 13.20	64 12 45.42	0.081	1	19.72	18.65	18.25	18.06	17.80	17.68	17.47	17.45	17.38	17.17	17.21	17.11	16.95	20.19	18.58	17.69	17.35	17.07	
240	17 14 44.66	64 13 16.54	0.076	1	19.42	18.50	18.23	17.97	17.75	17.60	17.43	17.30	17.22	17.07	17.09	17.03	17.12	20.17	18.43	17.59	17.22	17.00	
241	17 11 03.37	64 12 57.64	0.068	1	20.23	23.87	19.96	20.14	20.00	20.04	20.16	20.21	20.49	19.91	20.43	22.05	22.00	24.74	21.53	20.53	20.28	19.73	
242	17 15 34.81	64 13 41.64	0.078	2	20.36	19.30	18.98	18.84	18.57	18.49	18.39	18.41	18.20	18.10	18.05	18.21	18.24	20.27	19.13	18.47	18.23	18.12	
243	17 11 34.32	64 13 12.33	0.079	1	20.36	18.56	18.21	18.00	17.75	17.62	17.46	17.36	17.38	17.16	17.08	16.99	17.14	20.03	18.47	17.67	17.30	17.06	
244	17 13 57.69	64 14 15.56	0.079	1	18.56	18.77	18.49	18.25	18.09	17.99	17.84	17.68	17.58	17.47	17.62	17.31	17.17	20.75	18.86	17.99	17.57	17.32	
245	17 09 24.59	64 13 39.36	0.070	3	20.61	20.16	20.83	20.25	21.31	20.79	19.82	20.24	20.45	19.85	20.00	23.19	22.99	20.66	20.97	20.65	20.41	19.99	
246	17 13 42.79	64 14 32.73	0.079	2	20.40	19.10	18.62	18.44	18.13	18.07	17.83	17.85	17.66	17.56	17.44	17.50	17.31	20.86	18.93	18.06	17.67	17.32	
247	17 12 19.28	64 14 20.70	0.079	1	20.14	19.18	18.82	18.71	18.41	18.31	18.14	18.17	18.06	17.92	17.89	18.01	17.83	20.28	19.03	18.35	18.01	17.85	
248	17 13 48.84	64 14 37.97	0.081	6	99.00	21.23	20.72	20.44	19.71	20.60	19.80	20.61	19.90	19.34	19.30	22.71	22.00	21.52	20.44	20.09	19.86		
249	17 13 44.26	64 14 41.63	0.079	1	20.20	19.35	19.22	19.03	19.00	18.88	18.65	18.75	18.62	18.42	18.19	18.26	18.07	21.25	19.73	18.91	18.57	18.35	
250	17 13 24.08	64 15 13.93	0.086	2	19.82	18.62	18.30	18.20	18.04	17.90	17.68	17.61	17.58	17.43	17.47	17.34	17.26	19.80	18.54	17.87	17.58	17.37	
251	17 13 06.82	64 15 12.72	0.087	2	19.90	19.12	18.99	18.86	18.67	18.67	18.41	18.33	18.45	18.22	17.87	18.13	18.28	20.35	19.14	18.69	18.37	18.23	
252	17 15 52.55	64 15 33.15	0.081	1	21.77	20.78	20.15	20.25	20.04	19.63	19.73	19.62	20.03	19.87	20.58	20.94	19.90	23.23	21.03	19.98	19.65	19.36	
253	17 11 34.84	64 15 25.30	0.071	1	22.93	21.04	20.17	20.15	20.50	20.01	19.86	19.97	19.77	19.72	19.87	19.44	18.95	21.90	20.26	19.99	19.79	19.94	
254	17 09 14.21	64 14 59.26	0.085	3	16.50	15.62	15.45	15.44	15.19	15.13	15.03	15.02	15.01	14.93	14.91	14.90	14.91	16.81	15.64	15.16	14.97	14.96	
255	17 11 57.02	64 15 32.90	0.087	3	20.04	19.42	19.15	18.84	18.81	18.64	18.47	18.52	18.23	18.54	18.41	19.67	20.42	19.18	18.70	18.43	18.15		
256	17 10 46.23	64 15 38.78	0.079	2	21.00	19.89</																	

Table 4—Continued

No. (1)	R.A.(J2000) (2)	Decl. (3)	z_{phot} (4)	T (5)	b (6)	d (7)	e (8)	f (9)	g (10)	h (11)	i (12)	j (13)	k (14)	m (15)	n (16)	o (17)	p (18)	u' (19)	g' (20)	r' (21)	i' (22)	z' (23)	
266	17 12 26.13	64 20 16.30	0.090	1	20.74	19.31	18.91	18.58	18.25	18.11	17.93	17.89	17.90	17.65	17.68	17.49	17.50	20.93	19.04	18.18	17.80	17.63	
267	17 14 30.53	64 20 54.14	0.083	1	19.97	19.15	18.52	18.32	18.04	17.97	17.71	17.62	17.58	17.36	17.28	17.25	17.32	20.47	18.83	17.97	17.54	17.32	
268	17 12 21.50	64 20 38.16	0.078	1	21.45	20.76	20.23	20.09	19.80	19.72	19.48	19.41	19.34	19.18	19.14	19.24	19.25	22.51	20.82	19.72	19.31	19.02	
269	17 12 22.08	64 20 44.37	0.068	1	20.42	19.63	19.18	18.98	18.75	18.69	18.46	18.45	18.49	18.19	18.02	18.03	17.90	21.42	19.46	18.72	18.43	18.21	
270	17 12 56.44	64 20 55.33	0.079	1	19.93	18.66	18.39	18.15	17.86	17.74	17.51	17.48	17.44	17.22	17.30	17.05	16.86	20.52	18.67	17.77	17.38	17.11	
271	17 11 54.78	64 20 54.58	0.073	1	19.54	18.64	18.28	18.06	17.74	17.63	17.46	17.38	17.29	17.12	17.12	16.96	16.64	20.14	18.49	17.64	17.26	17.00	
272	17 10 42.05	64 20 46.45	0.070	3	20.65	20.65	20.64	20.14	20.75	20.53	20.62	20.07	20.11	21.52	21.11	24.58	99.00	20.76	20.31	20.39	20.26	20.83	
273	17 12 56.89	64 21 10.93	0.082	1	19.86	18.93	18.56	18.36	18.19	18.05	17.87	17.89	17.81	17.66	17.67	17.62	17.56	20.47	18.74	18.05	17.79	17.58	
274	17 14 24.12	64 21 26.94	0.079	1	21.09	20.31	19.60	19.50	19.16	18.99	18.84	18.89	18.87	18.78	18.52	18.68	19.26	21.61	19.96	19.12	18.73	18.45	
275	17 09 38.52	64 20 44.12	0.068	3	20.00	19.26	19.03	18.92	18.63	18.65	18.55	18.49	18.72	18.02	18.44	18.51	17.94	20.29	19.41	18.81	18.51	18.14	
276	17 16 20.72	64 22 15.44	0.082	3	20.82	19.78	19.35	19.16	19.03	18.87	18.69	18.66	18.54	18.43	18.38	18.36	18.04	20.54	19.50	18.89	18.51	17.97	
277	17 10 45.73	64 21 46.30	0.083	1	19.08	18.29	17.94	17.67	17.61	17.50	17.31	17.25	17.15	17.03	16.93	16.94	16.75	20.00	18.34	17.51	17.13	16.85	
278	17 15 54.64	64 22 58.43	0.084	3	15.56	14.57	14.37	14.25	14.03	13.93	13.83	13.81	13.78	13.73	13.70	13.70	13.70	16.04	14.51	13.95	13.74	13.69	
279	17 16 26.59	64 23 26.36	0.071	7	20.29	19.60	19.31	19.31	19.10	19.04	18.90	18.89	18.66	18.59	18.56	18.82	18.64	20.08	19.35	18.96	18.75	18.48	
280	17 10 50.36	64 22 50.85	0.087	3	18.93	18.15	18.02	17.88	17.68	17.58	17.48	17.48	17.45	17.31	17.45	17.28	17.28	17.46	19.14	17.99	17.60	17.42	17.35
281	17 16 25.38	64 23 46.90	0.087	3	20.09	19.33	19.20	18.89	18.81	18.74	18.49	18.41	18.44	18.35	18.22	18.52	18.24	20.62	19.22	18.74	18.40	18.23	
282	17 15 36.96	64 23 59.62	0.079	3	18.92	18.39	18.16	18.06	17.90	17.91	17.66	17.67	17.63	17.63	17.74	17.75	17.45	19.64	18.31	17.85	17.66	17.66	
283	17 10 08.46	64 23 25.29	0.090	7	19.00	18.60	18.48	18.39	18.25	18.19	18.10	17.78	18.07	17.95	17.73	18.17	18.16	19.21	18.52	18.24	17.98	17.91	
284	17 13 17.63	64 24 23.96	0.087	7	19.03	18.43	18.17	18.12	17.99	17.86	17.80	17.63	17.78	17.61	17.33	17.57	17.61	19.11	18.30	17.98	17.64	17.58	
285	17 14 26.06	64 24 36.01	0.083	1	19.70	18.78	18.33	18.10	17.83	17.69	17.51	17.42	17.34	17.20	16.94	17.04	16.98	20.21	18.56	17.69	17.32	17.07	
286	17 12 59.61	64 24 38.62	0.083	1	19.96	19.08	18.55	18.39	18.07	17.99	17.76	17.73	17.68	17.48	17.33	17.36	17.16	20.54	18.86	18.02	17.62	17.41	
287	17 15 59.20	64 25 45.34	0.073	4	20.64	20.65	20.25	20.04	20.19	19.59	19.48	19.33	19.56	18.90	19.33	19.14	19.99	21.54	20.28	19.68	19.43	19.10	
288	17 11 30.50	64 26 10.85	0.079	4	21.74	20.57	19.74	19.57	19.24	19.42	19.08	19.24	19.24	19.08	19.33	19.99	20.76	19.76	19.27	18.89	18.85		
289	17 14 48.87	64 26 45.24	0.083	1	21.86	20.46	20.01	19.99	20.01	20.02	19.40	19.42	19.45	19.27	19.76	19.75	19.99	23.69	20.37	19.80	19.57	19.24	
290	17 13 11.89	64 27 21.36	0.086	3	20.28	18.85	18.58	18.46	18.12	18.01	17.78	17.67	17.69	17.58	17.34	17.33	17.33	17.13	20.33	18.83	18.03	17.63	17.27
291	17 11 46.93	64 27 34.87	0.076	3	19.57	19.30	18.81	18.69	18.39	18.27	18.06	17.95	17.97	17.68	17.62	17.67	17.30	20.44	19.08	18.33	17.88	17.57	
292	17 15 42.89	64 29 31.74	0.073	2	20.02	19.64	19.25	19.08	19.00	18.96	18.77	18.55	18.57	18.24	18.25	18.92	17.96	21.41	19.53	18.92	18.58	18.33	
293	17 10 48.10	64 28 59.90	0.087	1	19.66	18.85	18.66	18.68	18.48	18.45	18.32	18.07	18.51	18.19	18.31	18.18	17.92	20.09	18.96	18.57	18.32	18.07	
294	17 08 39.96	64 29 17.21	0.068	3	16.18	15.52	15.36	15.36	15.16	15.12	15.05	15.05	15.13	15.03	15.04	15.02	15.07	16.59	15.55	15.19	15.05	15.05	
295	17 09 07.54	64 29 38.27	0.073	3	20.72	20.81	20.74	20.53	20.08	19.87	19.82	19.72	20.08	19.34	20.24	19.56	18.05	22.54	20.90	20.12	19.77	19.68	
296	17 15 08.12	64 30 42.35	0.078	3	19.55	19.25	18.91	18.75	18.50	18.31	18.22	18.19	18.07	17.66	17.78	17.83	17.75	20.10	19.15	18.44	17.93	17.81	
297	17 15 25.28	64 31 32.48	0.068	1	21.45	20.38	19.76	19.98	19.09	19.07	18.99	19.14	19.51	18.62	18.86	18.78	19.02	22.92	20.30	19.46	19.07	18.73	
298	17 09 36.70	64 30 40.87	0.068	5	19.89	19.82	19.35	19.36	19.08	19.11	19.07	18.81	19.20	18.89	18.74	19.04	18.75	20.56	19.58	19.23	19.02	18.86	
299	17 09 24.71	64 31 17.73	0.083	1	21.57	20.16	19.89	19.79	19.20	19.12	18.76	18.52	18.25	18.09	18.15	17.92	18.00	21.84	19.95	18.93	18.43	18.08	
300	17 09 13.34	64 31 31.46	0.076	1	19.94	18.95	18.50	18.35	17.95	17.85	17.69	17.67	17.60	17.42	17.40	17.24	17.10	20.25	18.79	17.89	17.54	17.21	
301	17 15 50.43	64 32 36.42	0.087	1	19.91	19.01	18.31	18.08	17.91	17.79	17.51	17.52	17.44	17.19	17.16	16.96	16.90	20.91	18.83	17.84	17.35	17.00	
302	17 15 46.50	64 32 49.38	0.069	3	18.72	20.00	18.87	19.38	19.17	19.57	19.08	19.27	18.89	18.64	19.22	19.01	20.26	22.02	19.78	19.34	19.09	18.94	
303	17 12 14.07	64 32 58.09	0.073	1	20.34	20.81	20.23	19.84	19.33	19.27	19.14	19.01	19.02	18.62	18.66	18.47	17.68	21.95	20.42	19.37	18.90	18.48	
304	17 11 43.05	64 33 00.48	0.068	1	20.09	18.32	18.07	18.00	17.47	17.31	17.12	17.07	17.01	16.84	16.91	16.77	16.69	20.49	18.32	17.32	16.97	16.73	
305	17 14 34.92	64 34 02.41	0.078	1	22.91	21.13	20.72	20.67	20.22	20.30	20.04	19.97	19.84	19.99	19.66	19.58	19.99	24.10	22.05	20.45	19.66	19.10	
306	17 15 20.03	64 34 15.10	0.083	1	20.71	19.25	18.68	18.60	18.23	18.13	17.94	17.95	17.83	19.99	17.52	17.52	17.20	20.60	19.02	18.17	17.79	17.54	
307	17 08 47.55	64 33 20.58	0.083	3	20.20	19.49	18.92	18.81	18.50	18.40	18.15	18.08	18.10	17.90	17.70	17.70	17.70	20.71	19.21	18.43	18.03	17.76	
308	17 09 21.01	64 33 35.03	0.083	3	19.67	19.15	18.72	18.63	18.36	18.19	18.00	17.86	17.92	17.73	17.69	17.50	17.44	20.17	19.03	18.25	17.83	17.52	
309	17 15 49.84	64 33 13.77	0.082	3	99.00	19.38	19.23	99.00	99.00	18.86	18.83	18.70	18.72	99.00	99.00	18.86	18.52	20.42	19.33	18.9			